ICHEP'98 #123
Submitted to Pa 1
Pl 1, 9

DELPHI 98-123 CONF 184
22 June, 1998

A precise measurement of the partial decay width ratio $R_b^0 = \Gamma_{b\bar{b}}/\Gamma_{had}$

Preliminary

DELPHI Collaboration

G.J.Barker[a], **G.Borisov**[b,1], **T.Hessing**[c], **R.McNulty**[a], **C.Mariotti**[a,2], **F.Martinez-Vidal**[d], **K.Mönig**[a], **A.M.Normand**[e]

Abstract

The partial decay width of the Z to $b\bar{b}$ quark pairs has been measured by the DELPHI detector at LEP using data taken in the years 1992–1995. B-hadrons, containing b-quarks, were tagged by several methods using either tracks with large impact parameters to the primary vertex complemented by event shape variables or reconstructed inclusive secondary vertices. Combining these methods in a Multivariate Analysis the value:

$$\frac{\Gamma_{b\bar{b}}}{\Gamma_{had}} = 0.21625 \pm 0.00067(\text{stat}) \pm 0.00061(\text{syst})$$

was found, where the $c\bar{c}$ production fraction was fixed to its Standard Model value.

Paper submitted to the ICHEP'98 Conference
Vancouver, July 22-29

[a] CERN, CH=1211 Geneva 23, Switzerland.
[b] CEA Saclay, DSM/DAPNIA, France.
[c] University of Oxford, England.
[d] IFIC, Universitat de València, Spain.
[e] University of Liverpool, England.
[1] On leave of absence from IHEP, Protvino, Russian Federation.
[2] On leave of absence from INFN, Italy.

1 Introduction

The relative decay width of the Z into b-quarks, $R_{\rm b}^0 = \Gamma_{\rm b\bar{b}}/\Gamma_{\rm had}$, plays an important role amongst the observables measured with high precision at LEP and SLC. The other observables are mainly sensitive to electroweak radiative corrections in the Z-propagator, setting important constraints on, for example, the Higgs boson mass [1]. However, these corrections mainly cancel in the ratio of two partial widths and only those to the $\rm Zq\bar{q}$ vertex remain. These corrections are naturally enhanced with the fermion mass and, since the b-quark is the isospin partner of the very heavy top-quark, the $\rm Zb\bar{b}$ vertex is especially interesting. As an example, within supersymmetry and for a certain range of the model's parameters, effects due to the existence of stop-quarks or charginos could lead to observable changes of $R_{\rm b}^0$ with respect to the Standard Model [2].

The presently published results from the LEP collaborations and SLD reach an overall accuracy of 0.5% [3, 4, 5, 6, 7, 8]; this accuracy is marginal to observe possible predicted deviations from the Standard Model. This paper updates and supersedes the previous DELPHI result and exploits the full statistics and understanding of the detector behaviour, improving significantly the precision of the previous measurement.

Experimentally, $R_{\rm b}^0$ can be obtained with only very small corrections from the ratio of cross-sections $R_{\rm b} = \sigma(\rm e^+e^- \to b\bar{b})/\sigma(e^+e^- \to hadrons)$. This paper presents three measurements of $R_{\rm b}$ using about 3.4 million hadronic events taken in the years 1992–1995 with the DELPHI detector at LEP. The data in 1992 and 1994 were collected at the centre of the Z peak; in 1993 and 1995, scans across the Z peak were performed.

All analyses compare the rates of events where only one or both of the b-quarks have been identified, from which $R_{\rm b}$ can be measured together with the b-tagging efficiency. Systematic errors due to the charm background and to hemisphere correlations have been considerably reduced with respect to previous analyses [5] due to improved tracking algorithms in the charged track reconstruction, to the use of new variables for the identification of b-quarks and to new methods for reconstructing the primary vertex. One analysis uses, in addition to the highly efficient and pure b-tag, additional tags for b-, c- and light quarks. All efficiencies apart from the background efficiencies of the primary b-tag are measured from data, so that the new tags reduce the statistical error without increasing the systematic uncertainties.

2 The DELPHI Detector

The DELPHI detector and its performance have been described in detail elsewhere [9, 10]. Only the details most relevant to this analysis are mentioned here and particular care is given to the new microvertex detector, installed in spring 1994, that allowed high values of purity and efficiency in the identification of the b-quarks to be reached.

In the barrel region, the charged particle tracks are measured by a set of cylindrical tracking detectors whose axes are parallel to the 1.2 T solenoidal magnetic field and to the beam direction.

The innermost one is the microvertex detector (VD), which is located between the LEP beam pipe and the Inner Detector (ID) [11, 12]. The DELPHI microvertex detector operational in the years 1991–1993 [11] was composed by 3 layers of single sided silicon microstrip detectors at radii of 6.3, 9 and 11 cm from the beam line, respectively called

the closer, inner and outer layers. To increase the performance of the detector in tracking and especially in the identification of B-hadrons, in 1994 it was upgraded using double sided silicon detectors to allow three dimensional impact parameter reconstruction. The microstrip detectors of the closer and outer layers provide hits in both the $R\phi$ and the Rz planes [1], while for the inner layer only the $R\phi$ coordinate is measured. For polar angles of $44^\circ \leq \theta \leq 136^\circ$ a track crosses all three silicon layers of the VD. The closer layer covers the polar region between 25° and 155°.

The measured intrinsic resolution is about 8 μm for the $R\phi$ coordinate for both the old and the upgraded VD, while for Rz it depends on the incident polar angle of the track and reaches about 9 μm for tracks perpendicular to the modules. For charged tracks with hits in all three $R\phi$ VD layers, the impact parameter resolution is $\sigma^2_{R\phi} = ((61/(P\sin^{3/2}\theta))^2 + 20^2)\mu\mathrm{m}^2$ for both the old and the upgraded VD and for tracks with hits in both Rz layers and with $\theta \approx 90^\circ$, $\sigma^2_{Rz} = ((67/(P\sin^{5/2}\theta))^2 + 33^2)\mu\mathrm{m}^2$.

The time projection chamber (TPC) is the main tracking device and is a cylinder of length 3 m, inner radius 30 cm and outer radius 122 cm. Between polar angles from 39° to 141°, tracks are reconstructed using up to 16 space points. Outside this region (21° to 39° and 141° to 159°), tracks can be reconstructed using at least 4 space points.

Additional precise $R\phi$ measurements are provided at larger and smaller radii by the Outer and Inner detectors respectively. The Outer Detector (OD) has five layers of drift cells at radii between 198 and 206 cm and covers polar angles from 42° to 138°. The Inner Detector (ID) is a cylindrical drift chamber having inner radius of 12 cm and outer radius of 28 cm and covers polar angles between 29° and 151° . It contains a jet chamber section providing 24 $R\phi$ coordinates, surrounded by five layers of proportional chambers giving both $R\phi$ and z coordinates.

The barrel electromagnetic calorimeter (HPC) covers polar angles between 42° and 138°. It is a gas-sampling device which provides complete three-dimensional charge information in the same way as a time projection chamber. The excellent granularity allows good separation between close particles in three dimensions and hence good electron identification even inside jets.

In the forward region the tracking is complemented by two sets of planar drift chambers (FCA and FCB), at distances of ±165 cm and ±275 cm from the interaction point. A lead glass calorimeter (EMF) is used to reconstruct electromagnetic energy in the forward region.

Muon identification in the barrel region is based on a set of muon chambers (MUB), covering polar angles between 53° and 127°. In the forward region the muon identification is provided using two sets of planar drift chambers (MUF) covering the angular region between 11° and 45°.

3 Event Selection

The criteria to select charged tracks and to identify hadronic Z decays were similar to those described in [5]. Charged particles were accepted if:

- their polar angle was between 20° and 160°,

[1] In the DELPHI coordinate system, z is along the beam line, ϕ and R are the azimuthal angle and radius in the xy plane, and θ is the polar angle with respect to the z axis.

- their track length was larger than 30 cm,
- their impact parameter relative to the interaction point was less than 5 cm in the plane perpendicular to the beam direction and less than 8 cm along the beam direction,
- their momentum was larger than 200 MeV/c with relative error less than 100%.

Neutral particles detected in the HPC were required to have measured energy larger than 700 MeV and those detected in the EMF greater than 400 MeV.

Events were then selected by requiring:

- at least 6 reconstructed charged particles,
- the summed energy of the charged particles had to be larger than 15% of the centre of mass energy, with at least 3% of it in each of the forward and backward hemispheres with respect to the beam axis.

The efficiency to find hadronic Z decays with these cuts was about 95% with only a very small bias towards a specific flavour, and all backgrounds were below 0.1%.

About 1.3 million hadronic Z decays were selected with two dimensional VD in 1992 and 1993, and 2.1 million hadronic Z decays from 1994 and 1995 data samples with the three dimensional VD. The ratio of the cross-section $Z \to b\bar{b}$ to the total hadronic cross-section varies very little at centre of mass energies close to the Z mass. Thus no selection on the centre of mass energy was made in 1993 and 1995. However the validity of this assumption has been tested (see section 7).

A sample about twice the data statistics of $Z \to q\bar{q}$ events was simulated using the Lund parton shower Monte Carlo JETSET 7.3 [13] (with parameters optimised by DELPHI) and the DELPHI detector simulation [10]. In addition dedicated samples of $Z \to b\bar{b}$ events were generated. The simulated events were passed through the same analysis chain as the real ones.

4 The Enhanced Impact Parameter Analysis

4.1 The method

Events are divided into hemispheres using the plane perpendicular to the thrust axis. If R_H is the fraction of hemispheres tagged as b and R_E is the fraction of events in which both hemispheres are tagged, R_b can be extracted by comparison of the rates of events where only one or both the b-quarks have been identified:

$$\begin{aligned} R_H &= R_\mathrm{b}\cdot\epsilon_\mathrm{b} + R_\mathrm{c}\cdot\epsilon_\mathrm{c} + (1 - R_\mathrm{b} - R_\mathrm{c})\cdot\epsilon_\mathrm{uds} \\ R_E &= R_\mathrm{b}\cdot\epsilon_\mathrm{b}^2\cdot(1+\rho) + R_\mathrm{c}\cdot\epsilon_\mathrm{c}^2 + (1 - R_\mathrm{b} - R_\mathrm{c})\cdot\epsilon_\mathrm{uds}^2, \end{aligned} \tag{1}$$

where ϵ_q is the efficiency to tag a hemisphere originating from a primary quark q (=uds, c, b) and the coefficient ρ accounts for hemisphere correlations in the tagging efficiencies for b-quarks. For the other quark species these correlation factors can safely be neglected due to the very high b-purity reached. If ρ, ϵ_c and ϵ_uds are calculated from the simulation and R_c is imposed from other measurements or from the Standard Model, R_b and ϵ_b can

be measured simultaneously from the data. Precise knowledge of the details of B-hadron decays is thus not required.

A new b-tagging algorithm was used. The main ingredient was the measurement of the track impact parameters. However it was complemented by additional information like the invariant mass and the energy of particles fitted to a secondary vertex. Where to cut in this variable is arbitrary and the cut chosen for the results was that which minimised the total error. Results are given as a function of the b-purity and b-efficiency of the data sample.

Two contributions to the systematic error are the background efficiencies and the hemisphere correlation coefficient ρ. The former can be substantially reduced using the purer tag. The second is the correlation between the two hemispheres in the event. From the previous analysis [5], it was estimated that the major contribution to this came from the common primary vertex. The correlation can be substantially reduced by computing a separate primary vertex for each hemisphere. The remaining correlation is discussed in section 4.4.

As the VD is essential for the measurement of the impact parameters in both the $R\phi$ and the Rz planes, the method was limited to events that have most of the tracks inside the acceptance of the VD. For this reason a cut of $|\cos\theta_{thrust}| < 0.65$ was applied.

For the extraction of $R_{\rm b}$ with such a method, a good description of the data by the simulation for the udsc-quarks is required. For this reason a fine tuning of the $R\phi$ and Rz impact parameter distributions in the simulation was developed and applied [14]. This led to substantially smaller uncertainties due to the understanding of the detector resolution.

4.2 Tagging technique

B-hadrons are significantly different from those containing only lighter quarks. They have a large mass, a long lifetime and a high decay multiplicity, they take more energy than light hadrons from the initial quark, etc. However in previous DELPHI measurements of $R_{\rm b}$, only their long lifetime and the high decay multiplicity were used for the tagging [5]. In this paper we describe a method of b-tagging which combines all these differences of the B-hadrons with respect to other particles into a single variable. The application of this method gives a significant improvement of the b-tagging efficiency with respect to the lifetime tag used previously.

The particles are clustered into jets (using JADE with y_{min}=0.01), since the jet axis is better than the thrust axis for giving an estimate of the initial quark direction. The hemisphere is then identified by the tagged jet. If more than one jet is in a hemisphere, the jet with the highest probability of coming from a b-quark is considered.

In this method, which is described in detail in [15], all discriminating variables are defined for jets with reconstructed secondary vertices; jets without reconstructed secondary vertices are not considered. Such a condition allows properties specific to B-hadrons to be used for the tagging and allows the separation of their decay products from those particles coming from b-quark hadronisation. In addition, the requirement of jets with reconstructed secondary vertices is a good selection by itself as it removes a significant part of the background. Thus hemispheres that would be tagged due to badly measured tracks with large impact parameters can be rejected by the vertex requirement. The purity of B-hadrons in jets with secondary vertices is about 85% with a selection efficiency of almost 50%.

The reconstructed secondary vertex is required to contain at least 2 tracks not compatible with the primary vertex and to have $L/\sigma_L > 4$, where L is the distance from the primary to the secondary vertex and σ_L is its error. Each track included in the secondary vertex should have at least one measurement in the VD and at least 2 tracks should have measurements in both the $R\phi$ and the Rz planes of the VD.

The description of the discriminating variables is as follows.

The jet lifetime probability, P_j^+, is constructed from the positively signed impact parameters of the tracks included in a jet and corresponds to the probability of a given group of tracks being compatible with the primary vertex [16, 17]. For jets with B-hadrons, this probability is very small due to the significant impact parameters of tracks from B decays. However, jets with c-quarks can also have low values of P_j^+ because of the non-zero lifetime of D-mesons, which limits the performance of the lifetime tag. The distribution of $-\log_{10}(P_j^+)$ for different quark flavours is shown in figure 1a.

The distribution of **the effective mass of particles included in the secondary vertex**, M_s, is shown in figure 1b. The mass of the secondary vertex for c-jets is limited by the mass of D-mesons and above $M_s = 1.8$ GeV/c^2 the number of vertices in c-jets decreases sharply, while that in b-jets extends up to 5 GeV/c^2.

The distribution of **the rapidity of tracks included in the secondary vertex with respect to the jet direction**, R_s^{tr}, is shown in figure 1c. Although a B-hadron has on average higher energy than a D-meson from a c-jet, the rapidities of particles from a B decay are on average less than those from a c-quark decay. This is explained by the higher mass of the B-hadron and the larger multiplicity of its decays. The secondary vertices in light quark jets are induced mainly by wrongly measured tracks. The wrong measurements occur due to multiple scattering in the detector, interaction in the material, etc so that tracks included in the secondary vertices of light quark jets are usually soft and their rapidity distribution is shifted to lower values.

The distribution of **the fraction of the charged energy of a jet included in the secondary vertex**, X_s^{ch}, for different quark types is shown in figure 1d. In the case of B-hadrons, when almost all particles included in the secondary vertex come from the B decay, the distribution of X_s^{ch} is determined by the fragmentation function $f(b \to B)$. The same is valid for c-quark jets where the distribution of X_s^{ch} is determined by $f(c \to D)$, which is softer than $f(b \to B)$. In light quark jets, the energy of the secondary vertex is much less than that in b-quark jets, as explained above.

For the combination of the discriminating variables, the following quantity is defined:

$$y = n_{\mathrm{c}} \cdot \prod \frac{f_i^{\mathrm{c}}(x_i)}{f_i^{\mathrm{b}}(x_i)} + n_{\mathrm{q}} \cdot \prod \frac{f_i^{\mathrm{q}}(x_i)}{f_i^{\mathrm{b}}(x_i)} = n_{\mathrm{c}} \cdot \prod y_i^{\mathrm{c}} + n_{\mathrm{q}} \cdot \prod y_i^{\mathrm{q}}, \qquad (2)$$

where n_{c} and n_{q} are the normalised number of jets with a reconstructed secondary vertex in $\mathrm{c\bar{c}}$ and $\mathrm{q\bar{q}}$ events respectively ($n_{\mathrm{c}} + n_{\mathrm{q}} = 1$) and $f_i^{\mathrm{q}}(x_i)$, $f_i^{\mathrm{c}}(x_i)$, $f_i^{\mathrm{b}}(x_i)$ are probability density functions of the variable x_i in uds-, c- and b-quark jets.

The products in (2) run over all tagging variables of a given jet. The variable R_s^{tr} is defined for each particle included in the secondary vertex and so the corresponding ratio of probabilities for each particle enters in equation (2). For the transformations $y_i^{\mathrm{c}}(x_i) = f_i^{\mathrm{c}}(x_i)/f_i^{\mathrm{b}}(x_i)$ and $y_i^{\mathrm{q}}(x_i) = f_i^{\mathrm{q}}(x_i)/f_i^{\mathrm{b}}(x_i)$ we use smooth functions which are obtained from a fit of the ratios of corresponding distributions. The jet is tagged as containing a b-quark if $y \leq y_0$, where the value y_0 can be varied to select the desired purity or efficiency of tagging.

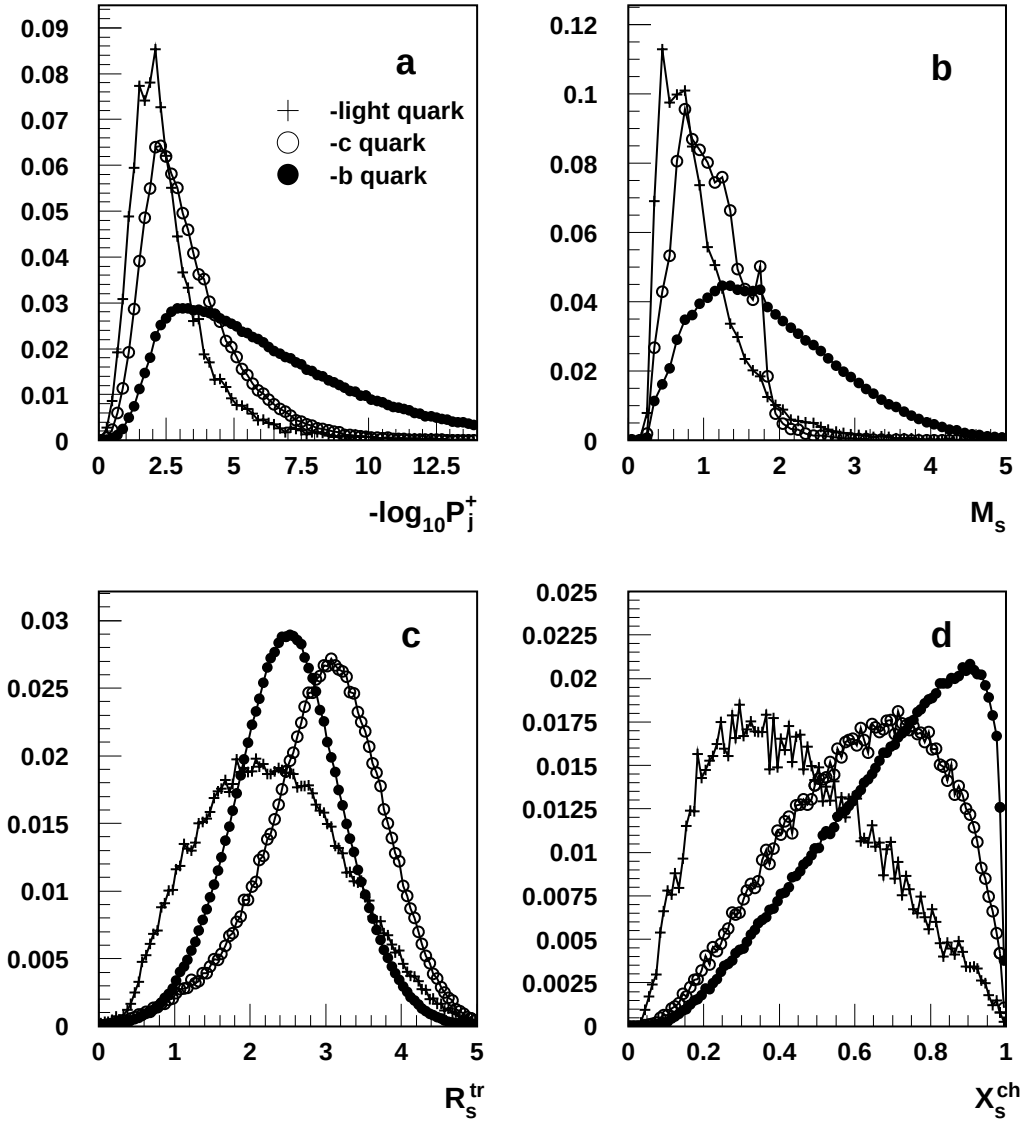

Figure 1: Distributions of discriminating variables used in the 'enhanced impact parameter' tagging.

Figure 2 shows the tagging efficiency versus purity of the selected sample for different combinations of discriminating variables. It can be seen that the addition of each new variable improves the tagging performance.

The enhanced tagging in comparison with the simple lifetime tag P_j^+ suppresses the background by more than a factor 3 for a b-tagging efficiency of 30% and about a factor 6 times for a b-tagging efficiency of 20%. A very pure b sample with purity more than 99.5% can be obtained with a b-efficiency of 20%.

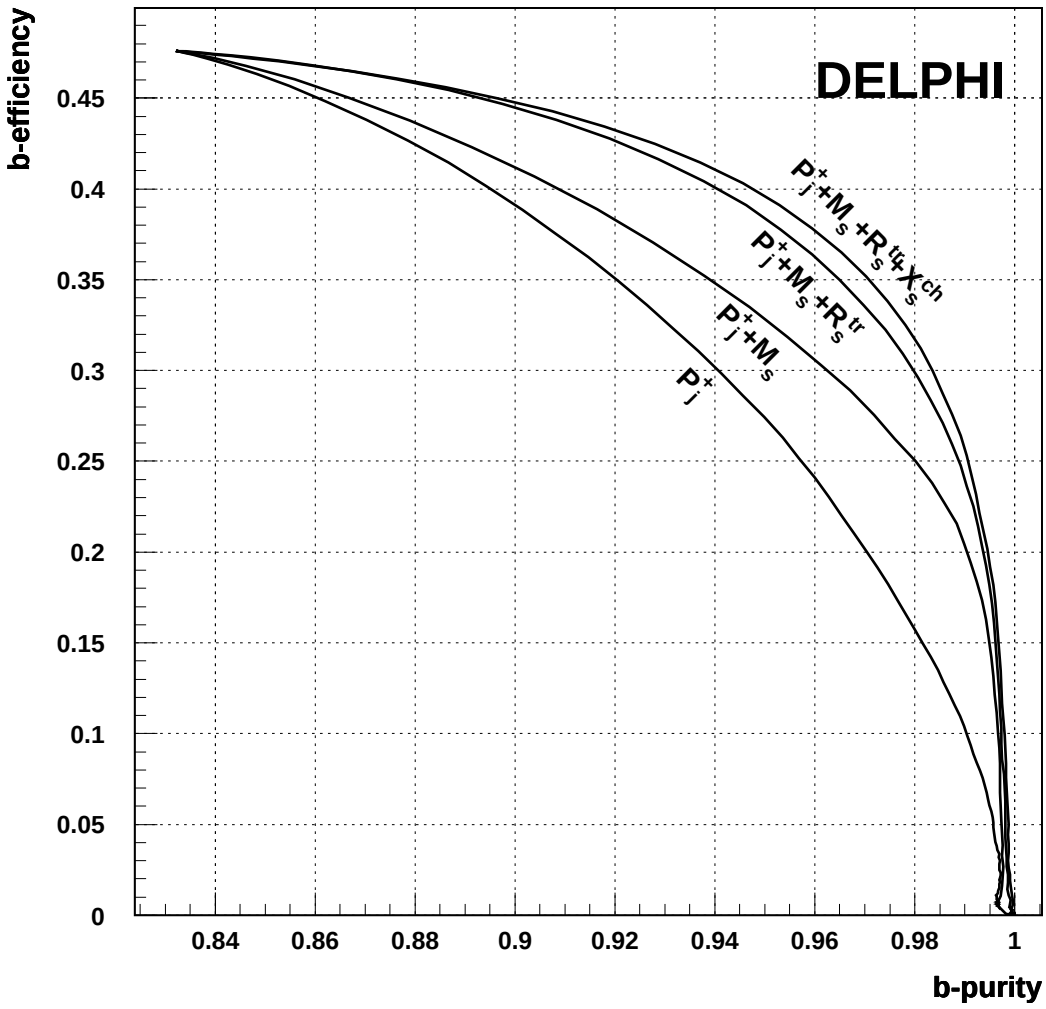

Figure 2: b-tagging hemisphere efficiency versus purity of selected sample of jets with reconstructed secondary vertices for different combinations of discriminating variables.

All distributions for this tagging method are taken from simulation, so that a check of their agreement with data is important for its successful application. For a measurement

of R_b, only the agreement of background distributions needs to be verified since the efficiency of b-quark tagging is taken from data.

The high purity of the tagged sample allows the extraction from data of the distributions of the discriminating variables for background and the comparison of them with those used in the simulation. B-hadrons in one hemisphere are tagged with a high purity of about 99% to give a clean and almost uncontaminated sample of B-hadrons in the opposite hemisphere. The distributions of the discriminating variables in such hemispheres can be subtracted after appropriate normalisation from the corresponding distributions in the untagged sample of jets with secondary vertices. These contain large contamination from other quark flavours and thus the distributions of discriminating variables for background can be obtained.

The comparison of these distributions in data and in simulation is shown in figure 3. Good agreement in the background description for all variables used in the tagging can be seen. Finally, figure 4 shows the comparison of distributions of the enhanced tagging variable $-\log_{10} y$, where y is defined by (2).

4.3 Light and charm quark efficiencies

The analysis was performed at many different values of the b-tagging efficiency and purity. The minimum total error (e.g. the sum in quadrature of the statistical and systematic errors) in the 1994–1995 data analysis was obtained for $\epsilon_b = 32.4\%$, i.e. for a cut on the variable $-\log_{10} y \geq 1$. For the two dimensional VD in 1992 and 1993 a lower efficiency of 28% is obtained for the same purity. The Multivariate Analysis (see Section 5), which uses the enhanced impact parameter tag as primary tag, has its optimum error at slightly harder cut values, namely $-\log_{10} y \geq 1.2$ for 1994–1995 and $-\log_{10} y \geq 0.6$ for 1992–1993. Since this section is mainly meant to illustrate the relevant features for the multiple tag analysis, which provides the main result for this paper, all numbers are presented using those cuts.

At these chosen working points, the tagging efficiencies for uds- and c-quarks were estimated using the simulation to be

$$\begin{aligned} \epsilon_{uds} &= 0.00050 \pm 0.00006 \\ \epsilon_c &= 0.00381 \pm 0.00025 \end{aligned} \tag{3}$$

for 1993 and 1992, while they are

$$\begin{aligned} \epsilon_{uds} &= 0.00052 \pm 0.00008 \\ \epsilon_c &= 0.00376 \pm 0.00027 \end{aligned} \tag{4}$$

for 1994 and 1995. The breakdown of the errors is given in table 1.

For most physics assumptions the recommendations of the LEPHF group [18] have been followed. The gluon splitting into $b\bar{b}$ quark pairs was recently measured [19, 20] allowing the two sources of heavy quark production from gluon splitting to be used independently, considerably reducing the systematic error due to these sources.

A specially complicated issue is the dependence of ϵ_c on the charmed hadron decay modes. For the b-tag used in this analysis roughly 45% of the tagged c-hemispheres contain a D^0 or D^+ each. About 10% contain a D_s and only 1% a charmed baryon. Details of the charmed baryon decays are therefore not important for the understanding

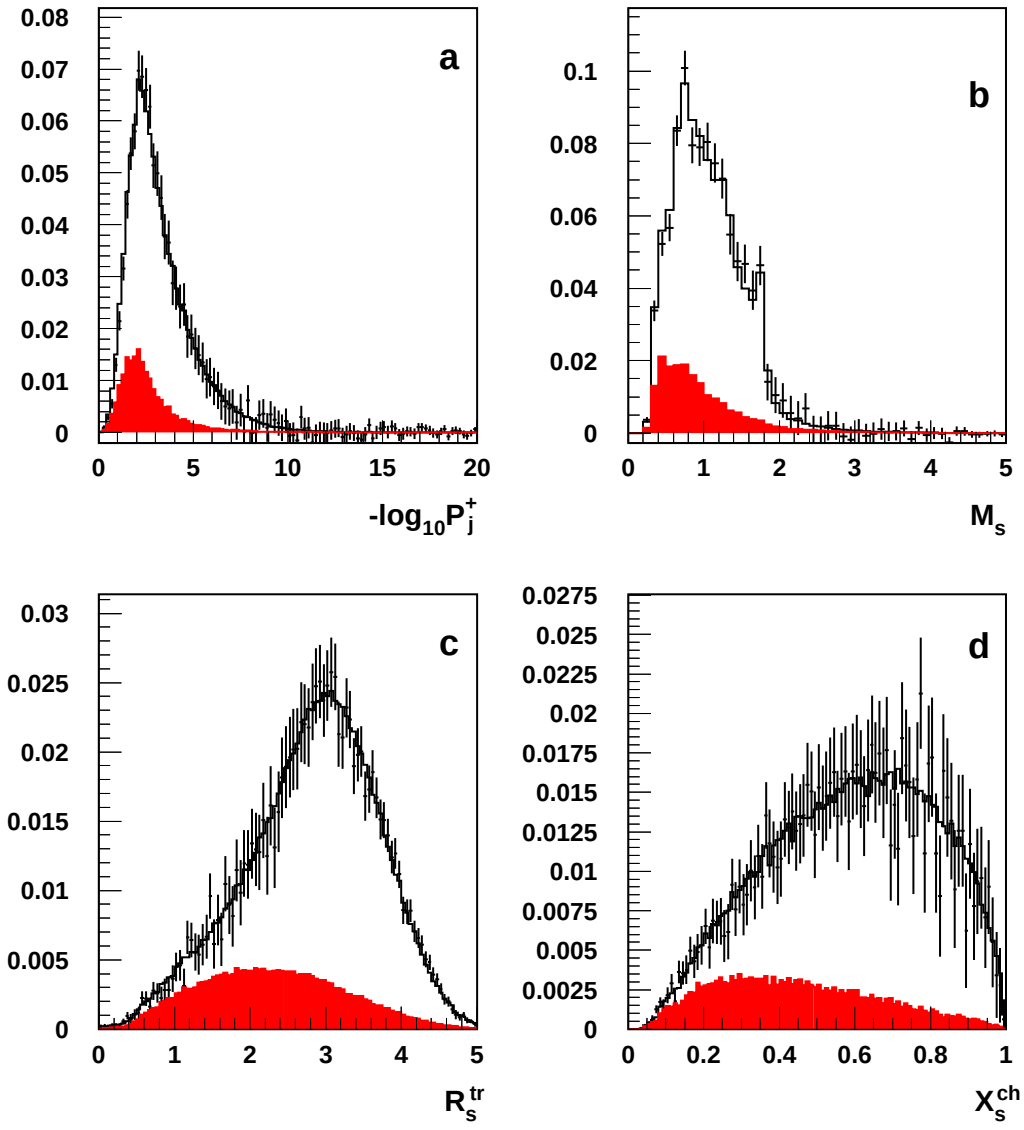

Figure 3: Distribution of discriminating variables for background (u,d,s,c) jets. The points with errors are from the data and the histogram is the simulation prediction. The contribution of light quark jets is shown as the filled histograms.

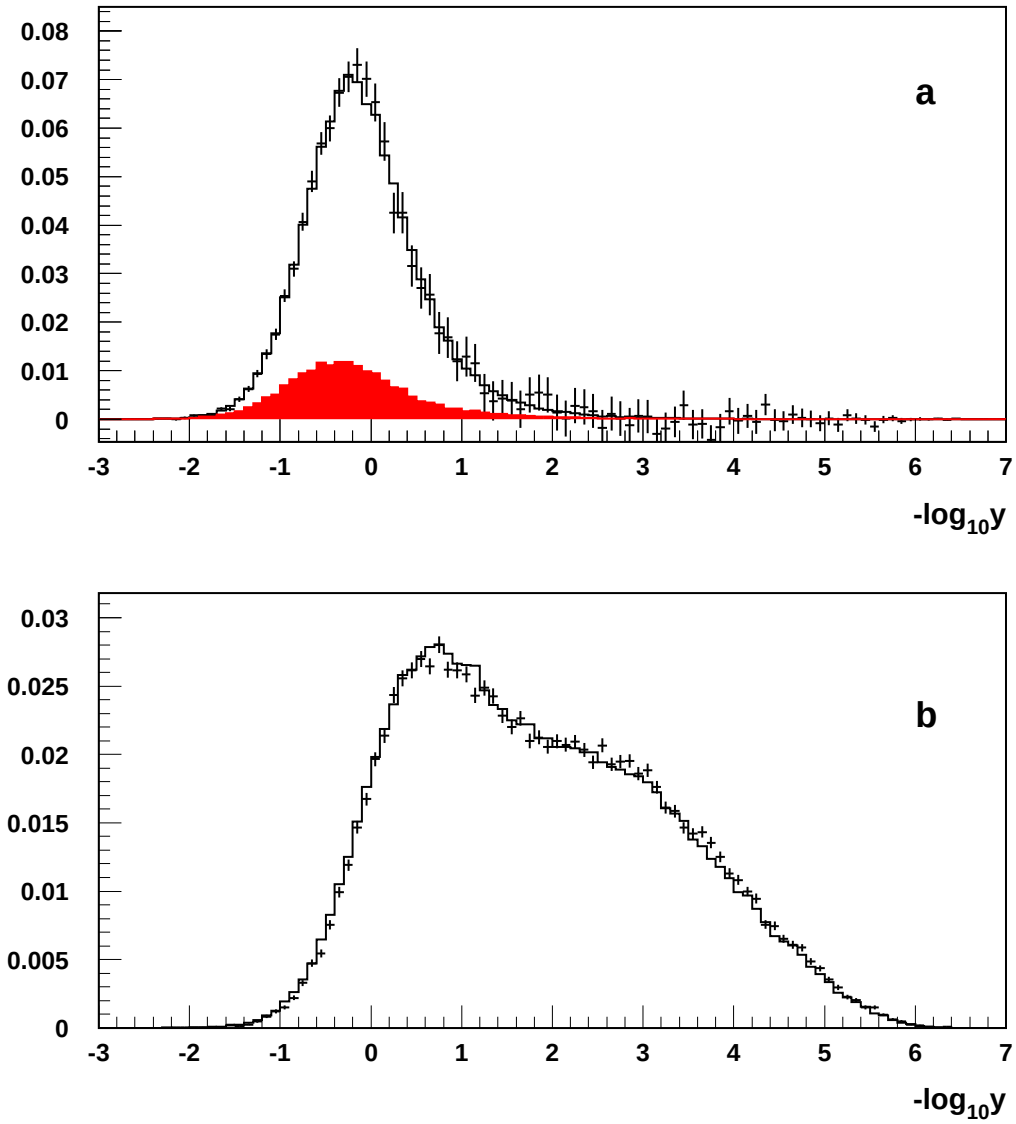

Figure 4: Distribution of the enhanced tagging variable $-\log_{10} y$ for (a) background (u,d,s,c) jets and (b) jets with b-quarks. The points with errors are from the data and the histogram is the simulation prediction. The contribution of light quark jets is shown as the filled histogram in the upper figure.

of ϵ_c. Because of the much worse knowledge of D_s decays compared to D^0 and D^+ the uncertainties due to the three charmed mesons are of comparable size. Two main features of D-meson decays are relevant for the c-tagging efficiency: the charged decay multiplicity and the multiplicity of neutral particles. The tagging efficiency rises with the charged multiplicity due to the better vertex finding efficiency and is almost zero for multiplicities less than two, where no vertex can be found. Since the invariant mass of the vertex is used in the tag, also the number of neutrals in the D decay is relevant. ϵ_c drops strongly from zero to one neutrals and significantly from one to more than one neutrals in the D decay.

The evaluation of the uncertainty due to the charge decay multiplicity is detailed in [18]. For D^0 and D^+ the relevant neutral multiplicities can be calculated from [21] to be:

$$\begin{aligned} \mathrm{BR}(D^0 \to \text{no neutrals}) &= (14.1 \pm 1.1)\% \\ \mathrm{BR}(D^0 \to 1\,\text{neut.}, \geq 2\,\text{charged}) &= (37.7 \pm 1.7)\% \\ \mathrm{BR}(D^+ \to \text{no neutrals}) &= (11.2 \pm 0.6)\% \\ \mathrm{BR}(D^+ \to 1\,\text{neut.}, \geq 2\,\text{charged}) &= (26.1 \pm 2.3)\% \end{aligned}$$

For the D_s it turns out that only the $\mathrm{BR}(D_s \to K^0X)$ is relevant. Adding up the exclusive modes with and without K^0 summarised in [21] a lower and upper limit of this branching ratio can be calculated from which $\mathrm{BR}(D_s \to K^0X) = (33 \pm 18)\%$ can be derived.

To estimate the uncertainty on ϵ_{uds} and ϵ_c due to detector effects, four tests were carried out.

- To estimate the effect of the resolution, the simulation was rerun with a tuning [14] that described the data worse than the default one (about 4% relative difference in the light and charm quark efficiencies).

- Another test to estimate the effect of the detector resolution on ϵ_c was the following: the resolution of the detector as estimated from the data was used in the definition of the tagging probability of simulated events. This second test was preferred for ϵ_c because it is sensitive to systematics related to the simulation of the charm background since charmed particles have a detectable lifetime and a non zero charged decay multiplicity. However it gave results consistent with the other method. For ϵ_{uds} it cannot be used, as it artificially modifies the tagging rate due to statistical fluctuations.

- To estimate the effect of correlations between tracks included in the probability (P_j^+) calculation, the difference in tagging rate between data and simulation using tracks with negative impact parameters was taken as the uncertainty on ϵ_{uds}.

- The VD track efficiency in the simulation was varied by the amount of the residual difference between the data and the Monte Carlo.

The errors obtained with the first, third and fourth tests were added in quadrature to obtain the final detector uncertainty on ϵ_{uds}. For ϵ_c only the second and fourth tests were used.

Source of systematics	Range	1992–1993		1994–1995	
		$\Delta\epsilon_{\mathrm{uds}}$ $\times 10^5$	$\Delta\epsilon_{\mathrm{c}}$ $\times 10^4$	$\Delta\epsilon_{\mathrm{uds}}$ $\times 10^5$	$\Delta\epsilon_{\mathrm{c}}$ $\times 10^4$
MC statistics		± 1.4	± 0.7	± 1.3	± 0.7
Detector resolution		± 1.3	± 1.2	± 3.3	± 1.3
Detector efficiency		± 1.0	± 0.8	± 1.0	± 0.8
K^0	Tuned JETSET$\pm$10%	± 0.6		± 0.6	
Hyperons	Tuned JETSET$\pm$10%	± 0.2		± 0.1	
Photon conversions	$\pm$50%	± 1.0		± 0.4	
Gluon splitting $g \to \mathrm{b\bar{b}}$	$(0.269 \pm 0.067)\%$	± 5.3	± 0.5	± 6.8	± 0.7
Gluon splitting $g \to \mathrm{c\bar{c}}$	$(2.33 \pm 0.50)\%$	± 1.2	± 0.1	± 2.3	± 0.2
D^+ fraction in $\mathrm{c\bar{c}}$ events	0.233 ± 0.027[1]		± 0.8		± 1.0
$\mathrm{D_s}$ fraction in $\mathrm{c\bar{c}}$ events	0.103 ± 0.029[1]		∓ 0.1		∓ 0.1
c-baryon fraction in $\mathrm{c\bar{c}}$ events	0.063 ± 0.028[1]		∓ 0.9		∓ 0.9
D decay multiplicity	see [18]		± 0.8		± 0.5
BR($\mathrm{D}^0 \to$ no neutrals)	$(14.1 \pm 1.1)\%$		± 0.4		± 0.5
BR($\mathrm{D}^0 \to 1$ neut., ≥ 2 charged)	$(37.7 \pm 1.7)\%$		± 0.2		± 0.2
BR($\mathrm{D}^+ \to$ no neutrals)	$(11.2 \pm 0.6)\%$		± 0.3		± 0.4
BR($\mathrm{D}^+ \to 1$ neut., ≥ 2 charged)	$(26.1 \pm 2.3)\%$		± 0.2		± 0.1
BR($\mathrm{D_s} \to \mathrm{K}^0\mathrm{X}$)	$(33 \pm 18)\%$		± 0.8		± 1.0
D^0 lifetime	0.415 ± 0.004 ps		± 0.2		± 0.2
D^+ lifetime	1.057 ± 0.015 ps		± 0.2		± 0.2
$\mathrm{D_s}$ lifetime	0.447 ± 0.017 ps		± 0.2		± 0.2
Λ_c lifetime	0.206 ± 0.012 ps		± 0.0		± 0.0
$\langle x_E(\mathrm{c}) \rangle$	0.484 ± 0.008		± 0.3		± 0.4
Total c physics			± 1.8		± 2.0
Total		± 6.0	± 2.5	± 8.1	± 2.7

Table 1: Systematic errors on the light and charm quark efficiencies at the working point of $\log_{10} y \geq 0.6$ for 1992-1993 and $\log_{10} y \geq 1.2$ for 1994-1995.
[1] Correlations between these sources are taken into account.

4.4 Hemisphere correlations

In the extraction of $R_{\rm b}$, one has to correct for the fact that the two hemispheres in an event are not completely uncorrelated and thus the double tag efficiency $\epsilon_{\rm q}^{(d)}$ is not exactly equal to the square of the hemisphere tagging efficiency. Due to the high purity, this effect can safely be neglected for non-b events. For the 1993 (1994) data analysis[2], it was estimated from the simulation to be $\rho = 0.0342 \pm 0.0047$ (0.0198 ± 0.0030) at the chosen working points.

Two main effects are responsible for ρ not being equal to zero:

- Angular effects: the particles in an event are typically nearly back to back. This leads to a positive correlation due to the polar angle. The multiple scattering contribution to the VD resolution increases with decreasing polar angle and close to the end of the VD some tracks get lost outside its acceptance. There are also some minor effects connected with the azimuthal angle. Due to the flatness of the beam-spot [3] at LEP, the resolution is better for horizontal than for vertical jets. Also, because of inefficient or poorly aligned modules, the detector is not completely homogeneous.

- QCD effects: as shown in figure 5 the b-tagging efficiency is a function of the momentum of the B-hadrons. Gluons emitted at large angles with respect to the quarks affect the energy of both quarks, leading to a positive correlation. In 2.2% of the events both b-quarks are boosted into the same hemisphere, recoiling against a hard gluon. This leads to a negative correlation.

To obtain the systematic error on the correlation estimate from the simulation, the fraction of tagged hemispheres was measured as a function of the relevant variable both in data and in simulation. From this, the correlation due to that single variable was calculated. This procedure uses the fact that the value of the test variable is correlated between the hemispheres, e.g. if one hemisphere has a cosine of its polar angle at $\cos\theta$ the other one has it at $-\cos\theta$. For the angular variables all events have been used. Due to the high purity of the tag and because the initial angular distributions are identical for b- and light quark events no bias was introduced. It was, however, verified that the conclusions did not change if a b-tag was required in the hemisphere opposite to the tested one. In all years a small difference ($\sim 0.15\%$) between data and the simulation has been found. Many tests have been done modifying the angular dependence of the b-tagging efficiency. Since always the changes in the angular correlation followed very closely the changes in the total correlation, the total correlation was corrected by half the difference between data and Monte Carlo taking as systematic error the squared sum of the full correction and the statistical error of the difference.

To test the correlation due to QCD effects, all events were forced to three jets and the jet momenta were recalculated using energy-momentum conservation. The momentum of the fastest jet (p_{jet}) was then defined as the test variable with the convention that it was counted positive in the one-jet hemisphere and negative in the two-jet hemisphere. Since the p_{jet} distribution is different for b and udsc events, a b-tag was required in the

[2] In the following some results will be given only for the 1993 and 1994 data analyses, one for each microvertex setup.

[3] Defined by the interaction points of a few hundred events within the same running period.

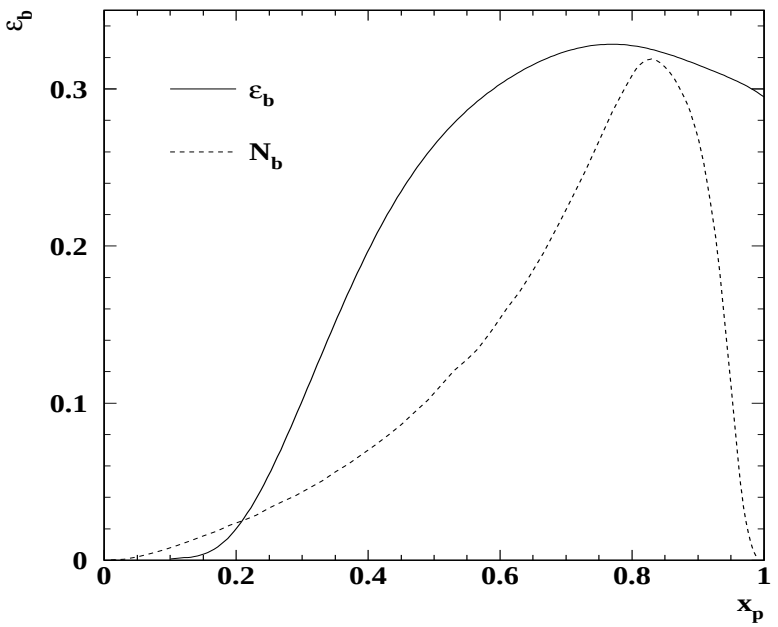

Figure 5: b-tagging efficiency as a function of the normalised B-hadron momentum (solid line). For comparison the dashed line shows the B-momentum spectrum with an arbitrary normalisation.

opposite hemisphere to avoid an artificial bias. As an additional complication, the two sources for QCD correlations act differently on the p_{jet} distribution. If the two b-quarks are in opposite hemispheres, the one-jet hemisphere represents the faster and thus better tagged b. If the two b-quarks are boosted into the same hemisphere, the one-jet side contains only a gluon. For that reason the one-jet hemisphere was only used if it passed a soft b-tag. On the two-jet side, a soft b-tag cannot be applied since this changes drastically the ratio of events with a fast b and a soft gluon and vice versa. As systematic uncertainty the maximum of the difference between the data and simulation measurements and the statistical error on this difference was taken. The systematic error induced by events with both b-quarks in one hemisphere was tested by varying their amount in simulation by 30%, as suggested by a comparison of the JETSET parton shower and second order matrix element simulations.

Figure 6 shows the correlations for the different sources obtained with this procedure in data and simulation as a function of the b-tagging efficiency. Also shown for the simulation is the sum of the different sources and the total correlation evaluated as $\rho = \frac{\epsilon_b^{(d)}}{\epsilon_b^2} - 1$. The agreement of the sum of the different sources with the total correlation indicates that no important source has been forgotten. Two b-quarks in the same hemisphere (negative correlation) would contribute here, slightly decreasing the sum of the components. To check this, the one-jet soft cut purity was moved in an attempt to get together different mixture from the two sources of QCD correlation. The central value of the p_{jet} correlation component was observed to increase with purity. It was however verified that the quoted

systematic error is insensitive to the one-jet soft cut purity.

Some additional physics systematics like B-lifetimes, decay multiplicities and fragmentation were also tested by reweighting the simulation. The B-hadron decay multiplicity was recently measured [22, 20] considerably reducing its error. However due to the use of separate hemisphere primary vertices, the effects of these additional physics systematics were found to be small. The uncertainties on ρ are summarised in table 2.

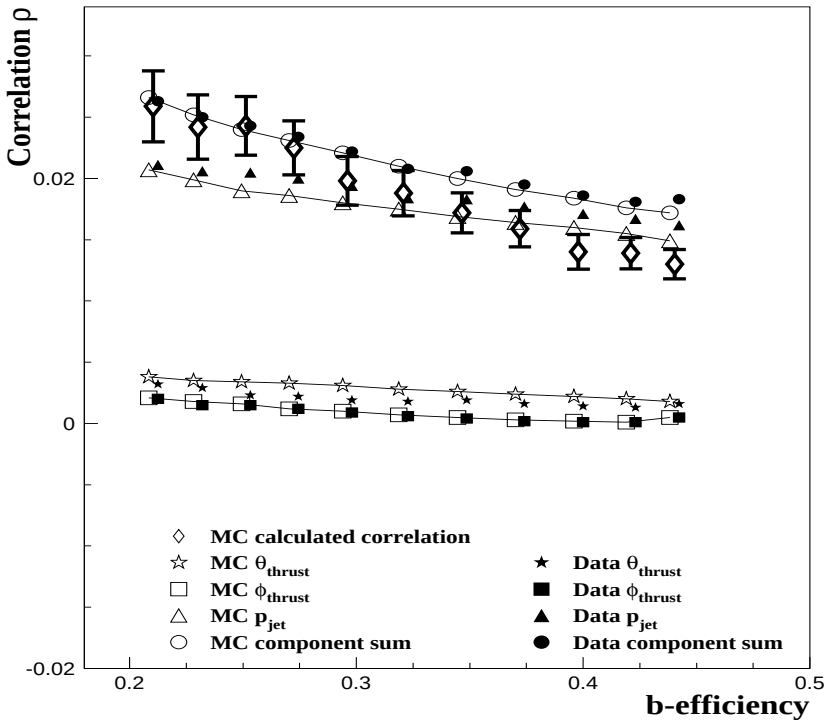

Figure 6: Hemisphere correlation due to the different sources and their sum as a function of the b-tagging efficiency for data and simulation. For the simulation also the total correlation is shown.

4.5 Results

Table 3 summarizes the number of hadronic Z decays selected in each year of operation, before and after the $\mid \cos\theta_{thrust} \mid$ cut. The numbers of single and doubly tagged hemispheres at the working points are also given. The bias towards b events in the selected sample was found to be small, $(1.51 \pm 0.09) \cdot 10^{-3}$, and was corrected for; its uncertainty is dominated by statistics.

Using the above values of the efficiencies and the correlation, with their errors, the measured value of R_{b} is:

$$R_{\mathrm{b}} = 0.21230 \pm 0.00211(\mathrm{stat}) \pm 0.00124(\mathrm{syst}) - 0.027(R_{\mathrm{c}} - 0.172) \quad (1992)$$
$$R_{\mathrm{b}} = 0.21836 \pm 0.00224(\mathrm{stat}) \pm 0.00111(\mathrm{syst}) - 0.028(R_{\mathrm{c}} - 0.172) \quad (1993)$$
$$R_{\mathrm{b}} = 0.21772 \pm 0.00131(\mathrm{stat}) \pm 0.00078(\mathrm{syst}) - 0.022(R_{\mathrm{c}} - 0.172) \quad (1994)$$
$$R_{\mathrm{b}} = 0.21653 \pm 0.00184(\mathrm{stat}) \pm 0.00107(\mathrm{syst}) - 0.024(R_{\mathrm{c}} - 0.172) \quad (1995)$$

Source of systematics	Range	$\Delta R_{\mathrm{b}} \times 10^4$ 1992–1993	1994–1995
MC statistics		± 6.06	± 3.81
Two b-quarks in same hemisphere	$\pm 30\%$	± 2.14	± 0.42
$\langle x_E(\mathrm{b}) \rangle$	0.702 ± 0.008	± 1.32	± 0.55
B decay multiplicity	4.97 ± 0.07	∓ 1.67	∓ 0.72
Average B lifetime	1.55 ± 0.04 ps	∓ 0.07	∓ 0.04
Angular effects	see text	± 3.36	∓ 0.71
Gluon radiation	see text	± 3.70	± 2.74
Total		± 8.42	± 4.85

Table 2: Systematic errors on hemisphere correlations for the Enhanced Impact Parameter Analysis.

Year	1992	1993	1994	1995	Total
Before $\mid \cos\theta_{thrust} \mid$ cut	696,520	660,288	1,367,437	664,493	3,388,738
After $\mid \cos\theta_{thrust} \mid$ cut	422,199	400,287	829,628	400,920	2,053,034
Single b-tags	45,192	42,620	108,629	52,282	248,723
Double b-tags	5,503	5,158	16,078	7,784	34,523

Table 3: Number of hadronic Z decays accepted for the analysis in each year of operation, before and after $\mid \cos\theta_{thrust} \mid < 0.65$ cut. The numbers of single and doubly tagged hemispheres are also given.

where the first error is statistical and the second one systematic. The explicit dependence of this measurement on the assumed R_c value is also given. These results have also been corrected for τ background. The results for the four years are compatible and can be combined, with the following assumptions:

- all statistical errors are assumed to be independent,
- the errors in the hemisphere correlations due to gluon radiation are assumed to be fully correlated,
- systematics from angular effects were assumed correlated for 1994–1995 and 1992–1993, but uncorrelated between them due to the independent microvertex configuration; the same was assumed for the detector effects on the estimate of light and charm quark efficiencies,
- the errors due to uds, c and b physics simulation inputs are assumed to be fully correlated.

With these assumptions, the result for the combined 1992–1995 data is:

$$R_b = 0.21670 \pm 0.00088(\text{stat}) \pm 0.00070(\text{syst}) - 0.024(R_c - 0.172) \quad (5)$$

where the $\chi^2/ndof$ of the combination is 4.5/3. The mean b-purity at the working point for this measurement is 98.5%.

The b hemisphere tagging efficiency was found to be for the 1993 (1994) data sample $\epsilon_b = 0.2383 \pm 0.0024$ (0.2946 ± 0.0017), compared to $\epsilon_b(MC) = 0.2302$ (0.2826) obtained from the simulation. The error is only due to the data statistics. In figure 7a the ratio of b-tagging efficiency in 1994 real data and in simulation is given as a function of the b-efficiency. The real data were about 4% more efficient than simulation. This difference is due to the poor knowledge of the b physics sector and is not coming from detector effects.

A breakdown of the error for the chosen cut on $-\log_{10} y$ is given in table 4.

As a cross-check of this measurement, a comparison of R_b as a function of the b-efficiency is given in figure 7b for the 1994 data sample. The measured value of R_b is stable over a wide range of b-efficiencies, and therefore of the purities and of the correlation.

5 The Multivariate Analysis

In the Enhanced Impact Parameter Analysis, hemispheres are tagged simply as b and non-b. This leads to two equations with six unknowns: R_b, ϵ_b, R_c, ϵ_{uds}, ϵ_c and ρ. Three of them, ρ and the efficiencies ϵ_{uds} and ϵ_c, are then taken from simulation and R_c is fixed to the Standard Model value. If the number of equations for physical observables was larger than the number of unknowns, the latter could be extracted directly from the data and the simulation would be required only to estimate systematic errors and the influence of hemisphere correlations. This is the principle of the multivariate approach to measuring R_b.

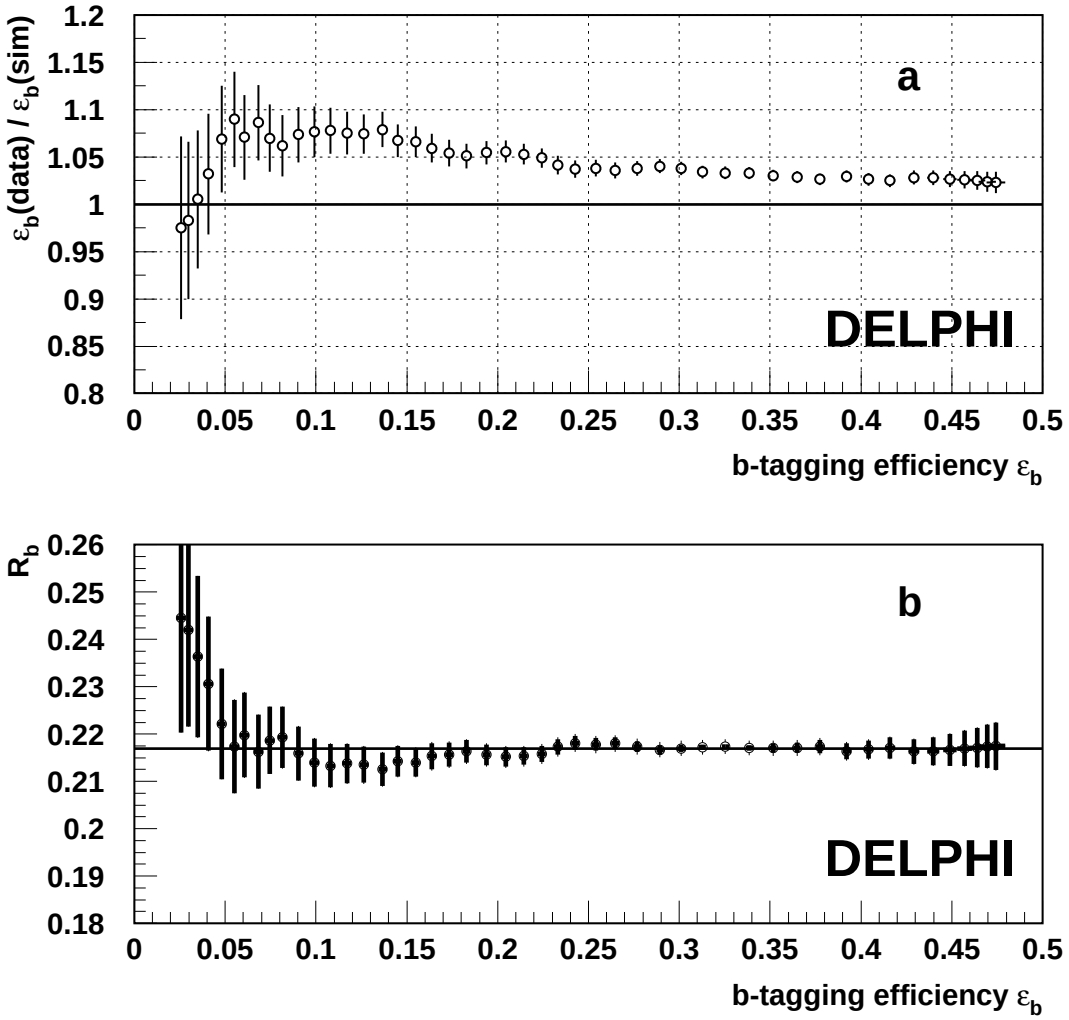

Figure 7: a) The ratio of the b-efficiency $\epsilon_{\rm b}$ measured in 1994 data and that taken from the simulation, as a function of the b-efficiency. b) The value of $R_{\rm b}$ with its total error as a function of the b-efficiency for 1994 data. The horizontal line corresponds to the value measured at the reference point, $-\log_{10} y \geq 1.2$, that corresponds to $\epsilon_{\rm b} = 29.5\%$.

	$\Delta R_{\rm b} \times 10^4$				
Error Source	1992	1993	1994	1995	Comb.
Statistical error	± 21.1	± 22.4	± 13.1	± 18.4	± 8.8
Simulation statistics	± 9.3	± 8.3	± 4.4	± 8.4	± 3.3
Light quark efficiency	± 2.8	± 2.9	± 3.1	± 2.7	± 3.0
Charm efficiency	± 3.4	± 3.6	± 2.8	± 3.1	± 3.1
Angular correlation	± 3.5	± 3.7	± 3.4	± 4.3	± 2.7
Gluon radiation	± 3.7	± 3.7	± 2.7	± 2.7	± 3.0
b physics correlation	± 3.0	± 3.0	± 1.0	± 1.0	± 1.6
Acceptance bias	± 2.3	± 1.8	± 1.3	± 2.2	± 0.9
Total systematic error	± 12.4	± 11.1	± 7.8	± 10.7	± 7.0
Total	± 24.5	± 25.0	± 15.2	± 21.3	± 11.2

Table 4: Sources of error for the measurement of $R_{\rm b}$ using the Enhanced Impact Parameter Analysis on all data sets and the combination.

5.1 The method

With some tagging algorithm, hemispheres of hadronic events containing $N_F = 3$ flavours (uds, c and b) are classified into N_T tagging categories or tags. The set of observables is then the matrix d_{IJ} with I,J = 1,...,N_T, defined as the observed fraction of events tagged as I and J for hemispheres 1 and 2 respectively. The corresponding expected fraction of events t_{IJ} can be written as

$$t_{IJ} = \sum_{\rm q} \epsilon_{\rm q}^I \epsilon_{\rm q}^J (1 + \rho_{\rm q}^{IJ}) R_{\rm q}. \tag{6}$$

In equation (6), $R_{\rm q}$ are the flavour fractions, satisfying $\sum_{\rm q} R_{\rm q} = 1$, and $\epsilon_{\rm q}^I$ is the probability to classify a hemisphere of flavour q (=uds, c, b) as tag I. The matrix $\rho_{\rm q}^{IJ}$ accounts for hemisphere-hemisphere tagging correlations for flavour q and tags I and J. Assuming that all the hadronic hemispheres are classified as one of the tags, the conditions

$$\sum_I \epsilon_{\rm q}^I = 1, \quad {\rm q} = {\rm uds, c, b} \tag{7}$$

and

$$\sum_I \epsilon_{\rm q}^I \epsilon_{\rm q}^J \rho_{\rm q}^{IJ} = 0, \quad {\rm q} = {\rm uds, c, b}; \quad J = 1, ..., N_T \tag{8}$$

are satisfied. The $N_T(N_T+1)/2 - 1$ independent measurements are therefore described by the following set of unknown independent parameters: $(N_F - 1)$ flavour fractions, $N_F(N_T - 1)$ efficiencies and $N_F N_T(N_T - 1)/2$ correlation coefficients. As hemisphere correlations are kept small, the independent correction factors $\rho_{\rm q}^{IJ}$ for $I, J \neq N_T$ can be taken from simulation[4]. Thus the global counting of degrees of freedom requires at least

[4] We consider as linearly dependent correlations all coefficients having at least one N_T tag. In principle, any other tag could be considered as dependent. However, at is will be explained in section 5.2, the N_T category will correspond to a no-tag category containing all hemispheres not classified in any other tag. As a consequence it has the most complex mixture of flavours being statistically significant and thus correlations containing it are preferred to be determined from the fit to data.

$N_T = 6$ for a constraint fit. The fit of the d_{IJ} observables to equation (6), satisfying (7) and (8), should provide, in principle, the full efficiency matrix $\epsilon_{\rm q}^I$ together with the flavour fractions $R_{\rm q}$ and the correlation coefficients $\rho_{\rm q}^{IJ}$ for I or J equal to N_T. The method of Lagrange multipliers is appropriate to solve this problem [23, 24]. However, in practice, the solution to this problem is not unique [25] and additional constraints are needed. In the analysis presented here, the problem is resolved if the uds- and c-quark backgrounds of a b-tagging category are calculated from Monte Carlo simulation, fixing $R_{\rm c}$ to its electroweak theory prediction. Systematic dependences of $R_{\rm b}$ on these three parameters can be reduced if the corresponding b-tag has a high b-purity (b-tight tag in the following) [26]. As detailed below, the enhanced impact parameter b-tag used in the previous analysis will be used to provide the b-tight tag. This tag will have the highest effect on the analysis, and all the other tags (two additional b-tags, one charm and one uds) will provide additional constraints to improve the error and to cross-check the analysis. The systematic error will reflect the uncertainties in the simulation calculations of the background efficiencies of the b-tight tag, $\epsilon_{\rm uds}^{\rm b-tight}$ and $\epsilon_{\rm c}^{\rm b-tight}$, and the correlations $\rho_{\rm q}^{IJ}$ with $I, J \neq N_T$. The result will be given as a function of the assumed value of $R_{\rm c}$. Even though the smallest number of tags to measure $R_{\rm b}$ is now $N_T = 4$, the choice $N_T = 6$ was made in order to overconstrain the problem and to minimize the error. The number of independent observables is therefore 20 with 14 independent unknowns: 13 efficiencies and $R_{\rm b}$.

5.2 The hemisphere multiple tag

To provide the six hemisphere tags, the enhanced lifetime tag used in the Enhanced Impact Parameter Analysis and defined by equation (2) is complemented with two additional flavour tagging algorithms. The tags are constructed in an attempt to isolate uds-, c- and b-quarks with high efficiency and purity, using exclusively the information provided by each hemisphere. In particular, the primary vertex is reconstructed in all the tagging methods independently in the two hemispheres, so the hemisphere correlations are kept small.

The *multivariate flavour tagging* algorithm [26] is based on the large mass and relatively long lifetime of B-hadrons and some event shape properties of its decays. All the available information is combined using multivariate techniques. The lifetime information exploits the large impact parameters of tracks coming from B decays together with a search for secondary vertices and their invariant masses. Finally, the lifetime information is combined with event shape properties of the B decays like large transverse momentum of the tracks with respect to the jet axis, rapidity distributions and the boosted sphericity. A total of $N = 13$ variables is finally adopted. A detailed description of the variables is provided in reference [26].

The probabilities $p_{\rm q}^\lambda$ of observing a value of the variable λ for a hemisphere of flavour q are computed using model distributions taken from simulation. An estimate of the relative probability to observe simultaneously a set of N variables is given by

$$\mathcal{P}_{\rm q} = \frac{n_{\rm q} \prod_{\lambda=1}^{N} p_{\rm q}^\lambda}{\sum_{\rm q'} n_{\rm q'} \prod_{\lambda=1}^{N} p_{\rm q'}^\lambda}, \tag{9}$$

where $n_{\rm q} = 1$ for ${\rm q} = {\rm c}, {\rm b}$ and $n_{\rm q} = 3$ for ${\rm q} = {\rm uds}$ hemispheres. The empirical factor 3 assigned to uds reflects the fact that this flavour is the sum of the three lighter flavours

u, d and s, which are taken together because their distributions are similar. With this formulation the 5 flavours have the same weight.

In practice, what counts in comparing flavours are ratios of probabilities or differences of their logarithms. For this reason new estimators $\mathcal{L}_{\rm q}$, called flavour likelihoods, are introduced. $\mathcal{L}_{\rm b}$ is defined as

$$\mathcal{L}_{\rm b} = \frac{2\ln\mathcal{P}_{\rm b} - \ln\mathcal{P}_{\rm uds} - \ln\mathcal{P}_{\rm c}}{\sqrt{6}} \tag{10}$$

and similarly for $\mathcal{L}_{\rm uds}$ and $\mathcal{L}_{\rm c}$. A hemisphere can be classified according to the largest flavour likelihood (which is positive).

Similarly to the multivariate approach, the *flavour confidences* method [27] is based not only on the track impact parameters but also on two other kinematic variables, the track momentum and the angle with respect to the jet axis. The method uses the simulation to build a function $\mathcal{C}_{\rm q}$ which gives the fraction of tracks coming from uds-, c and b-quarks in a bin of three particle characteristics: impact parameter over its error, momentum and angle to the jet axis. Possible kinematic effects in the decay of B-hadrons produce correlations between the three quantities which are automatically taken into account by the three-dimensional binning. The individual flavour confidences are finally combined to make the hemisphere tag:

$$\mathcal{CONF}_{\rm q} = \frac{n_{\rm q}\prod_i \mathcal{C}^i_{\rm q}}{\sum_{\rm q'} n_{\rm q'}\prod_i \mathcal{C}^i_{\rm q'}}, \tag{11}$$

$\mathcal{C}^i_{\rm q}$ being the q flavour confidence for track i.

Although some track information (in particular impact parameters, momentum and angle to the jet axis) is used in both tags, multivariate and confidences, it is used differently and the overlap is checked not to be complete. Thus interesting gains in performances can be obtained in a suitable mixture. The method of combination which was found to be the best of several investigated was a simple linear combination for each flavour:

$$\Delta_{\rm q} = (1-\alpha)\mathcal{L}_{\rm q} + \alpha\ln(1-\mathcal{CONF}_{\rm q}) \tag{12}$$

The quantities $\Delta_{\rm q}$ are called flavour multivariate discriminators and are the final basis of the classification. In principle, a different value of α could be used for each flavour, but it turns out that the same value ($\alpha = 0.8$) optimizes the three flavours. The apparently high ratio $\alpha/(1-\alpha) = 4$ is due to the fact that the range of values of the multivariate flavour likelihood is larger than that for the flavour confidences; it corresponds to approximately equal weights for the two components. Figure 8 shows the distributions of the flavour multivariate discriminators for data and simulation where the level of agreement can be seen within three orders of magnitude. The analysis is insensitive to small disagreements as they affect only the efficiencies, which are fitted from data. The effects on the correlation are discussed in section 5.4.

The definition of the tags is given in table 5. Three of the six tags are designed to identify b-quarks, one c-quarks and one uds-quarks. Finally the no-tag category contains all hadronic hemispheres not classified in one of the previous tags, in order to satisfy condition (7). To avoid double counting, the hemisphere tags defined in order of decreasing priority.

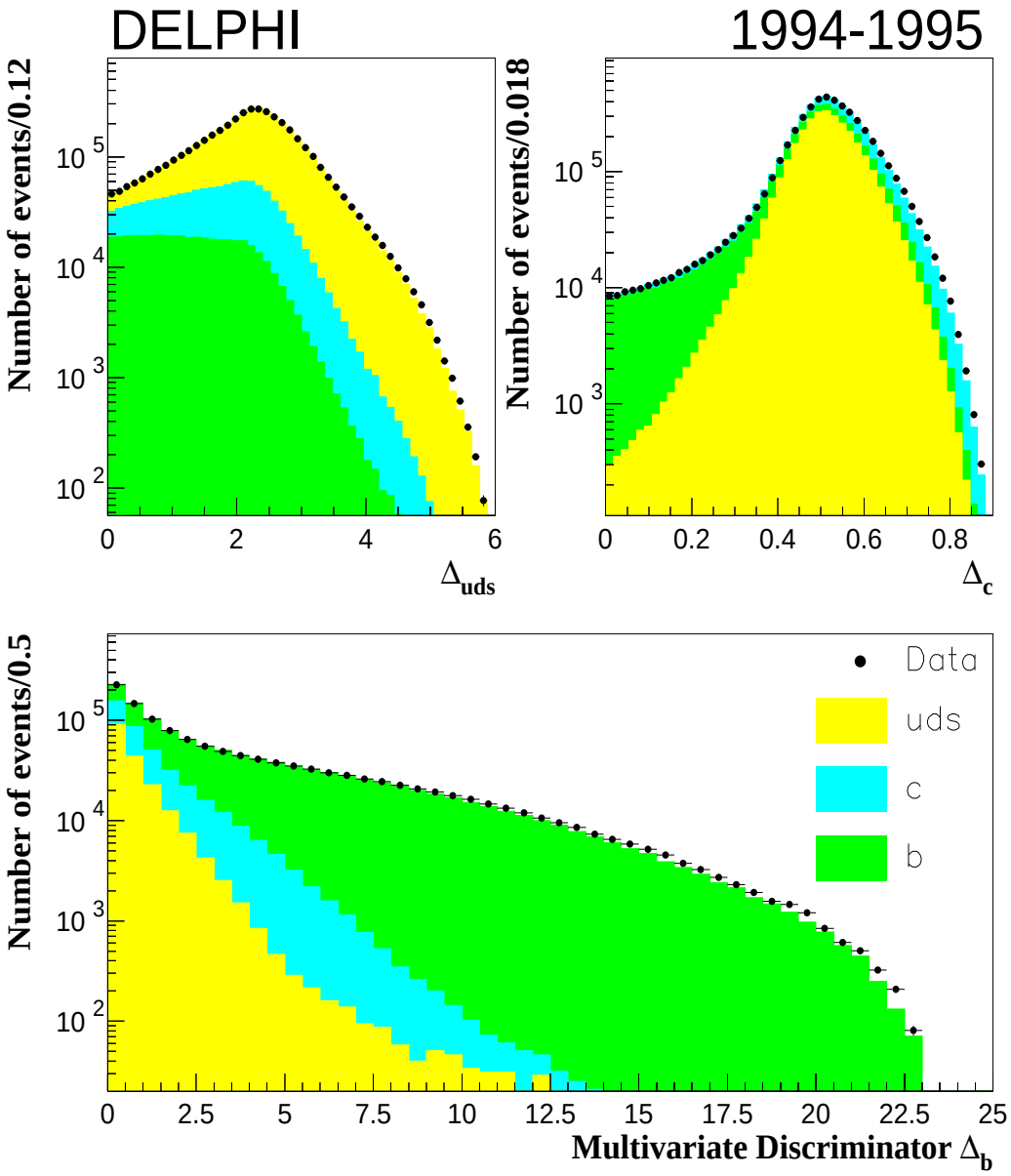

Figure 8: Distribution of the multivariate discriminator Δ_q in the uds, c and b tags for 1994–1995 data and simulation. The different types of shading show the different flavour contributions to the simulated event sample. The simulation distributions are normalized to the data statistics.

Tag	Condition	Priority	Cut values	
			1992–1993	1994–1995
b-tight	$y \leq y_0$	6	0.6	1.2
b-standard	$\Delta_{\rm b} \geq \Delta_{\rm b,0}^{high}$	5	3.5	3.5
b-loose	$\Delta_{\rm b} \geq \Delta_{\rm b,0}^{low}$	4	1.4	1.2
charm	$\Delta_{\rm c} \geq \Delta_{\rm c,0}$	3	0.58	0.65
uds	$\Delta_{\rm uds} \geq \Delta_{\rm uds,0}$	2	2.7	3.2
no-tag		1		

Table 5: The hemisphere tags defined in order of decreasing priority.

The b-tight tag has the strongest influence on $R_{\rm b}$ and the cut $-\log_{10} y_0$ was fixed at 1.2 in 1994–1995 and 0.6 in 1992–1993 to minimize the total error. All other cuts are chosen in order to obtain good efficiencies with reasonable backgrounds in the relevant tags. They are given in table 5. The Monte Carlo expectations for the efficiencies are given separately for 1993 and 1994 in table 6. This table is a measurement of the performance of the tags and tagging techniques all together. In this analysis of $R_{\rm b}$, only the charm and light quark backgrounds of the b-tight tag are taken from simulation. Therefore the light and charm quark systematic errors of the Enhanced Impact Parameter Analysis are valid for this measurement of $R_{\rm b}$. All the other efficiencies are measured directly from the data and can be used as a cross-check of the analysis (see table 6 and table 8).

	1993			1994		
Tag I	$\epsilon_{\rm uds}^I$	$\epsilon_{\rm c}^I$	$\epsilon_{\rm b}^I$	$\epsilon_{\rm uds}^I$	$\epsilon_{\rm c}^I$	$\epsilon_{\rm b}^I$
b-tight	0.00050	0.00381	0.23003	0.00052	0.00376	0.28236
b-standard	0.00188	0.02631	0.17051	0.00126	0.02692	0.15578
b-loose	0.01446	0.07754	0.16043	0.01219	0.07858	0.15158
charm	0.05814	0.16428	0.05704	0.04942	0.15617	0.04963
uds	0.11977	0.03579	0.00548	0.11819	0.03025	0.00471
no-tag	0.80530	0.69226	0.37649	0.81856	0.70431	0.35591

Table 6: Simulation results for the tagging efficiencies at the nominal cuts for 1993 and 1994.

Compared with the Enhanced Impact Parameter Analysis in which only b-tight tagged hemispheres are used, in the Multivariate Analysis all hadronic hemispheres are tagged, allowing the statistical accuracy to be increased. As it will be shown in section 5.5, the systematic uncertainty on $R_{\rm b}$ is also improved.

5.3 The measurement of $R_{\rm b}$

The experimentally measured numbers for the different categories of doubly tagged events which passed the $|\cos\theta_{thrust}|$ cut are given in table 7 for the 1993 and 1994 analyses.

The fit of $R_{\rm b}$ and the efficiencies to these numbers gives the following results for each year of operation:

$$R_{\rm b} = 0.21273 \pm 0.00164(\text{stat}), \quad \chi^2/ndof = 5.28/6 \quad (1992)$$
$$R_{\rm b} = 0.21727 \pm 0.00171(\text{stat}), \quad \chi^2/ndof = 7.52/6 \quad (1993)$$

	1993					
Tag	b-tight	b-standard	b-loose	charm	uds	no-tag
b-tight	5,158					
b-standard	7,405	2,762				
b-loose	6,839	5,070	2,764			
charm	2,568	2,388	4,196	4,026		
uds	268	416	1,408	5,504	4,068	
no-tag	15,224	14,204	22,719	47,804	51,151	194,345
	1994					
Tag	b-tight	b-standard	b-loose	charm	uds	no-tag
b-tight	16,078					
b-standard	17,049	4,564				
b-loose	16,261	9,017	5,025			
charm	5,737	4,150	7,386	6,757		
uds	662	766	2,583	9,877	9,210	
no-tag	36,764	25,527	43,749	88,319	109,031	411,116

Table 7: Measured numbers of doubly tagged events, passing the $|\cos\theta_{thrust}|$ cut in 1993 and 1994.

$$R_{\rm b} = 0.21681 \pm 0.00099(\text{stat}), \quad \chi^2/ndof = 4.95/6 \quad (1994)$$
$$R_{\rm b} = 0.21591 \pm 0.00145(\text{stat}), \quad \chi^2/ndof = 2.04/6 \quad (1995)$$

The errors are only statistical. The efficiencies obtained from the same fits for 1993 and 1994 are shown in table 8. They can be compared with the simulation predictions of table 6. For a complete comparison, an estimate of the systematic errors must be included.

5.4 Systematic errors

The systematic errors are due to the quantities estimated from simulation: event selection bias, light and charm quark backgrounds in the b-tight tag and hemisphere correlations.

5.4.1 Light and charm quark efficiency uncertainties

The sensitivity of $R_{\rm b}$ to light and charm quark efficiency uncertainties is the same as in the Enhanced Impact Parameter Analysis. The sensitivity to backgrounds is quantitatively defined by the relative change of $R_{\rm b}$ due to the change of the background efficiency,

$$\frac{\Delta R_{\rm b}}{R_{\rm b}} \frac{\epsilon_{\rm b}^{\rm b-tight}}{\Delta\epsilon_{\rm uds}^{\rm b-tight}}, \qquad \frac{\Delta R_{\rm b}}{R_{\rm b}} \frac{\epsilon_{\rm b}^{\rm b-tight}}{\Delta\epsilon_{\rm c}^{\rm b-tight}}. \tag{13}$$

In this analysis they have been estimated to be -5.7 and -1.5 for light and charm quarks respectively. They have been estimated in section 4.3, where table 1 shows the breakdown of these uncertainties into the different sources.

5.4.2 Hemisphere correlation uncertainties

The $\rho_{\rm q}^{IJ}$ hemisphere correlation corrections as estimated from simulation for the 1994 analysis together with their sensitivities are given in the second column of table 9, where

	1993		
Tag I	$\epsilon^I_{\rm uds}$	$\epsilon^I_{\rm c}$	$\epsilon^I_{\rm b}$
b-tight	0.00050	0.00381	0.2389 ± 0.0022
b-standard	0.0026 ± 0.0007	0.0238 ± 0.0033	0.1747 ± 0.0014
b-loose	0.0135 ± 0.0006	0.0805 ± 0.0048	0.1605 ± 0.0016
charm	0.0731 ± 0.0008	0.1798 ± 0.0037	0.0574 ± 0.0014
uds	0.1267 ± 0.0015	0.0327 ± 0.0045	0.0052 ± 0.0005
no-tag	0.7837 ± 0.0020	0.6794 ± 0.0085	0.3633 ± 0.0024
	1994		
Tag I	$\epsilon^I_{\rm uds}$	$\epsilon^I_{\rm c}$	$\epsilon^I_{\rm b}$
b-tight	0.00052	0.00376	0.2960 ± 0.0015
b-standard	0.0019 ± 0.0004	0.0240 ± 0.0019	0.1575 ± 0.0009
b-loose	0.0125 ± 0.0006	0.0787 ± 0.0028	0.1494 ± 0.0010
charm	0.0614 ± 0.0006	0.1692 ± 0.0023	0.0512 ± 0.0008
uds	0.1291 ± 0.0006	0.0309 ± 0.0023	0.0050 ± 0.0003
no-tag	0.7947 ± 0.0011	0.6935 ± 0.0047	0.3410 ± 0.0015

Table 8: Tagging efficiencies with statistical errors for data as measured from the fit at the nominal cuts for 1993 and 1994. For a complete comparison of the fit results with the simulation, an estimate of the systematic error must be included. Errors given in this table include data and simulation statistics.

the errors are due to simulation statistics. Only the relevant correlations with a sensitivity higher than 0.010 are shown. The sensitivity is defined as the relative change on $R_{\rm b}$ due to a change of a given correlation, $\frac{\Delta R_{\rm b}}{R_{\rm b}\Delta\rho^{IJ}_{\rm q}}$. The sensitivity of this measurement of $R_{\rm b}$ to $\rho_{\rm b}^{\rm b-tight,b-tight}$ is 0.767 for 1994–1995 and 0.693 for 1992–1993, compared to unity in the Enhanced Impact Parameter Analysis. However, as shown in the table, there are other correlations with important sensitivities which have zero sensitivity in the Enhanced Impact Parameter Analysis. As explained in section 5.1, correlations containing the no-tag category (I or $J = N_T$, which have a complex mixture of flavours being statistically significant) were determined from the fit to data, so they have a negligible sensitivity on the analysis.

Systematic errors on $\rho^{IJ}_{\rm q}$ arise from uncertainties in the simulation both of uds, c and b physics and of the vertex detector acceptance and gluon radiation.

Uncertainties in physical parameters used in the simulation of correlations are calculated by varying these physics inputs within their experimental ranges around their central values, according to the prescription given in reference [18]. For each variation of these physical parameters, obtained by reweighting the simulation, all the correlation correction factors are recomputed, allowing a new determination of $R_{\rm b}$. The change observed on $R_{\rm b}$ is assigned as systematic error. Table 10 summarizes the errors on $R_{\rm b}$ due to these physical uncertainties. The correlation between uds and charm efficiency uncertainties and hemisphere-hemisphere correlations due to physics inputs are small enough that it can be neglected.

Remaining errors on the correlations not due to physics simulation can be estimated by isolating the contributions to correlations and comparing their effect in data and simulation. The variables used to isolate the correlation sources are exactly the same as

			$\cos\theta_{thurst}$			ϕ_{thurst}			p_{jet}		
	MC global	Sensitivity	MC	RD	D	MC	RD	D	MC	RD	D
b correlations											
$\rho_{\mathrm{b}}^{\mathrm{b-tight,b-tight}}$	0.0198 ± 0.0020	0.767	0.0031	0.0019	0.0002	0.0010	0.0009	0.0009	0.0180	0.0194	0.0007
$\rho_{\mathrm{b}}^{\mathrm{b-tight,b-standard}}$	0.0034 ± 0.0020	0.219	0.0013	-0.0003	0.0003	-0.0008	-0.0009	0.0010	0.0184	0.0195	0.0005
$\rho_{\mathrm{b}}^{\mathrm{b-tight,b-loose}}$	0.0031 ± 0.0020	0.107	0.0004	-0.0002	0.0002	-0.0017	-0.0014	0.0003	0.0098	0.0104	0.0005
$\rho_{\mathrm{b}}^{\mathrm{b-tight,charm}}$	0.0047 ± 0.0039	-0.041	-0.0042	-0.0026	0.0025	0.0027	0.0009	0.0004	-0.0175	-0.0179	0.0012
$\rho_{\mathrm{b}}^{\mathrm{b-standard,b-standard}}$	0.0073 ± 0.0037	-0.081	0.0032	0.0035	0.0005	0.0003	-0.0006	0.0005	0.0183	0.0179	0.0010
$\rho_{\mathrm{b}}^{\mathrm{b-standard,b-loose}}$	0.0034 ± 0.0031	-0.088	0.0033	0.0033	0.0004	0.0006	-0.0016	0.0008	0.0106	0.0118	0.0006
$\rho_{\mathrm{b}}^{\mathrm{b-standard,charm}}$	0.0042 ± 0.0058	0.023	-0.0129	-0.0115	0.0010	-0.0004	-0.0001	0.0001	-0.0104	-0.0082	0.0013
$\rho_{\mathrm{b}}^{\mathrm{b-loose,b-loose}}$	0.0095 ± 0.0038	-0.047	0.0038	0.0029	0.0005	0.0012	-0.0012	0.0010	0.0082	0.0085	0.0007
$\rho_{\mathrm{b}}^{\mathrm{b-loose,charm}}$	-0.0079 ± 0.0059	0.014	-0.0137	-0.0112	0.0009	-0.0011	-0.0001	0.0001	-0.0242	-0.0272	0.0011
c correlations											
$\rho_{\mathrm{c}}^{\mathrm{b-standard,charm}}$	0.0015 ± 0.0173	0.014	-0.0100	-0.0078	0.0003	0.0018	0.0014	0.0003	0.0133	0.0088	0.0007
$\rho_{\mathrm{c}}^{\mathrm{b-loose,charm}}$	0.0028 ± 0.0097	0.024	-0.0135	-0.0106	0.0003	0.0005	0.0001	0.0001	0.0146	0.0167	0.0011
$\rho_{\mathrm{c}}^{\mathrm{charm,charm}}$	0.0434 ± 0.0080	-0.013	0.0183	0.0095	0.0002	0.0021	-0.0001	0.0001	0.0117	0.0168	0.0007
uds correlations											
$\rho_{\mathrm{uds}}^{\mathrm{charm,uds}}$	0.0134 ± 0.0078	0.020	0.0093	0.0092	0.0006	-0.0012	-0.0009	0.0002	0.0182	0.0174	0.0007
$\rho_{\mathrm{uds}}^{\mathrm{uds,uds}}$	0.0758 ± 0.0057	0.034	0.0079	0.0091	0.0007	0.0048	0.0042	0.0004	0.0383	0.0339	0.0012

Table 9: b, c and uds correlations with major sensitivity (> 0.010) on R_{b} at the nominal cuts for the 1994 data. The individual contributions to the total correlation for the data (RD) and for the simulation (MC) are shown, together with the statistical error on their difference (D).

Source of systematics	Range	$\Delta R_{\rm b} \times 10^4$ 1992–1993	1994–1995
MC statistics		± 5.58	± 3.77
Two b-quarks in same hemisphere	$\pm 30\%$	± 0.66	± 0.44
$\langle x_E(\mathrm{b}) \rangle$	0.702 ± 0.008	± 1.77	± 1.00
B decay multiplicity	4.97 ± 0.07	∓ 1.46	∓ 0.65
Average B lifetime	1.55 ± 0.04 ps	∓ 0.03	∓ 0.03
Gluon splitting $g \to \mathrm{c\bar{c}}$	$(2.33 \pm 0.50)\%$	± 0.12	± 0.12
Gluon splitting $g \to \mathrm{b\bar{b}}$	$(0.269 \pm 0.067)\%$	∓ 0.13	∓ 0.13
Charm physics	see table 1	± 0.65	± 0.44
Angular effects		± 2.51	± 0.71
Gluon radiation		± 2.38	± 2.65
Total		± 7.02	± 4.86

Table 10: Systematic errors due to hemisphere correlations for the Multivariate Analysis.

described in the Enhanced Impact Parameter Analysis: the polar and azimuthal angles and p_{jet}.

The contribution to $\rho_{\rm q}^{IJ}$ from one of the above variables Θ can be determined through the following expression:

$$\rho_{\mathrm{q},\Theta}^{IJ} = \frac{\int d\Theta f_{\rm q}(\Theta) \left[\epsilon_{\rm q}^{I,same}(\Theta)\epsilon_{\rm q}^{J,oppo}(\Theta) \; + \; \epsilon_{\rm q}^{J,same}(\Theta)\epsilon_{\rm q}^{I,oppo}(\Theta)\right]}{2\left[\int d\Theta f_{\rm q}(\Theta)\epsilon_{\rm q}^{I,same}(\Theta)\right] \; \left[\int d\Theta f_{\rm q}(\Theta)\epsilon_{\rm q}^{J,same}(\Theta)\right]} - 1, \qquad (14)$$

where $f_{\rm q}(\Theta)$ is the fraction of hemispheres of flavour q as a function of the variable Θ and $\epsilon_{\rm q}^{I,same}(\Theta)$ and $\epsilon_{\rm q}^{I,oppo}(\Theta)$ are the efficiencies to tag a hemisphere of flavour q as a function of Θ in the same and opposite hemisphere respectively.

The contribution $\rho_{\mathrm{q},\Theta}^{IJ}$ can easily be computed for the simulation where the flavour q is known. However, comparison of data and simulation requires the experimental isolation of this flavour in the data. This flavour isolation was obtained successfully for uds- and b-quarks using a soft multivariate tag, but not for c-quarks due to the small charm event statistics and the rather poor c-quark purity. However, the quoted systematics uncertainties were not affected because of the small sensitivity of $R_{\rm b}$ to c correlations. The b and uds selections were achieved by imposing the cuts $\Delta_{\rm b} > 3.3$ (3.0) and $\Delta_{\rm uds} > 2.9$ (3.3) in 1992–1993 (1994–1995) on the opposite hemisphere to the tested one. These cuts were chosen to achieve hemisphere b- and uds-purities of about 92%. In addition, as described in section 4.4, to reduce the effect of two b-quarks boosted into the same hemisphere, when testing the correlation due to QCD effects, the one-jet hemisphere was only used if it passed a soft multivariate tag of purity about 76% ($\Delta_{\rm b} > 0.9$ in 1992–1993 and $\Delta_{\rm b} > 0.6$ in 1994–1995). Table 9 gives the results of this procedure for all relevant correlation coefficients in 1994, for data and simulation. Figure 6 shows the total b-tight tag correlation as a function of the b-tight tag efficiency, together with each of the three components and their sum as obtained with this procedure, for simulation and data.

The systematic error for the QCD and the angular correlation was finally estimated as in the Enhanced Impact Parameter Analysis. The errors from the three sources were added

quadratically and the quoted uncertainties are listed in table 10. It must be stressed that this systematic error cannot be attributed only to differences between data and simulation for the particular flavour, but they can also be due to imperfections of the procedure, in particular the flavour isolation.

5.5 Results and consistency checks

From all previous numbers, the final results for each data sample are the following:

$$R_{\rm b} = 0.21273 \pm 0.00164(\text{stat}) \pm 0.00109(\text{syst}) - 0.026(R_{\rm c} - 0.172) \quad (1992)$$
$$R_{\rm b} = 0.21727 \pm 0.00171(\text{stat}) \pm 0.00100(\text{syst}) - 0.029(R_{\rm c} - 0.172) \quad (1993)$$
$$R_{\rm b} = 0.21681 \pm 0.00099(\text{stat}) \pm 0.00069(\text{syst}) - 0.022(R_{\rm c} - 0.172) \quad (1994)$$
$$R_{\rm b} = 0.21591 \pm 0.00145(\text{stat}) \pm 0.00100(\text{syst}) - 0.024(R_{\rm c} - 0.172) \quad (1995)$$

These results should be compared with the Enhanced Impact Parameter Analysis results of section 4.5. It can be seen that they are compatible taking into account uncorrelated error differences.

The results for the four years are compatible and can be combined, with the same assumptions as detailed in section 4.5. The result for the combined 1992–1995 data is:

$$R_{\rm b} = 0.21605 \pm 0.00067(\text{stat}) \pm 0.00061(\text{syst}) - 0.024(R_{\rm c} - 0.172) \quad (15)$$

where the $\chi^2/ndof$ of the combination is 4.0/3. As previously, the mean b-purity at the working point for this measurement is 98.5%.

Figures 9 and 10 show the stability of the final $R_{\rm b}$ result as a function of the b-tight tag efficiency for the 1994–1995 and 1992–1993 combinations respectively, together with the contributions to the total error. It can be seen that the minimum error is obtained at a b-efficiency of 29.6% (i.e. for a cut $-\log_{10} y \geq 1.2$) in 1994–1995, and of 27.1% (cut $-\log_{10} y \geq 0.4$) in 1992–1993. However, to have similar purities in all years and to minimize our error in the data combination, the cut $-\log_{10} y \geq 0.6$ was taken for 1992–1993, which corresponds to a b-efficiency of 23.9%.

Figure 11 shows the stability of $R_{\rm b}$ as a function of all other hemisphere b-standard, b-loose, charm and uds tag efficiencies for 1994–1995. Table 11 reports a breakdown of the error on this measurement. From the direct comparison of this table with table 4 it is concluded that both statistical errors and systematic uncertainties coming from hemisphere correlations are improved.

6 Secondary Vertex Analysis

An independent analysis was carried out on the 1992–1995 data sets using only reconstructed vertex information for the tagging of b quarks. The multihadronic event selection and the impact parameter fine tuning were in common with the Enhanced Impact Parameter and Multivariate analyses.

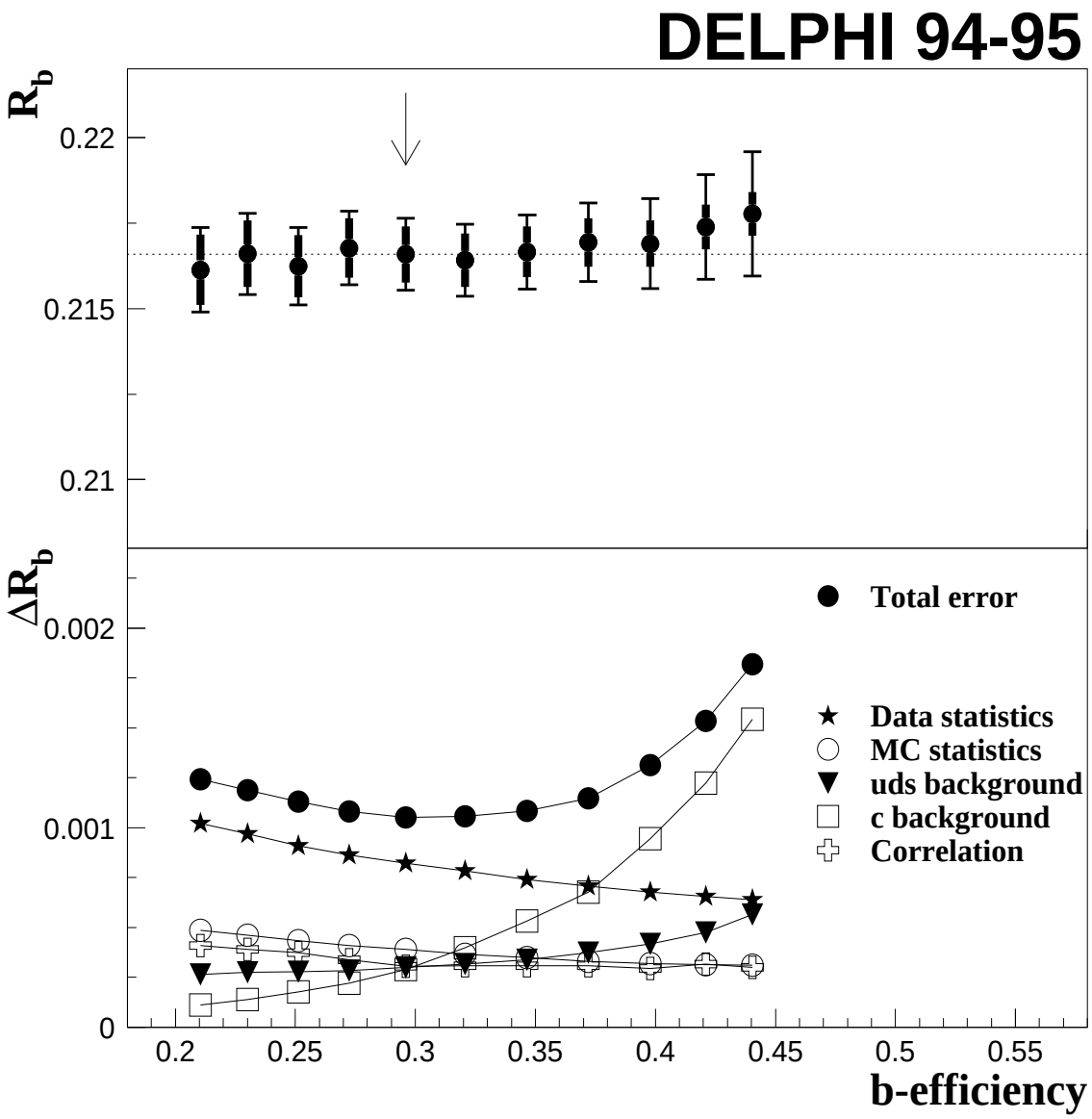

Figure 9: Stability of the 1994–1995 R_b result as a function of the b-tight tag efficiency, together with the contributions to the total error. The minimum error is obtained at an efficiency of 29.6%, where the b-purity is 98.5%. In the upper plot the thick error bar represents the statistical uncertainty and the narrow one is the total error.

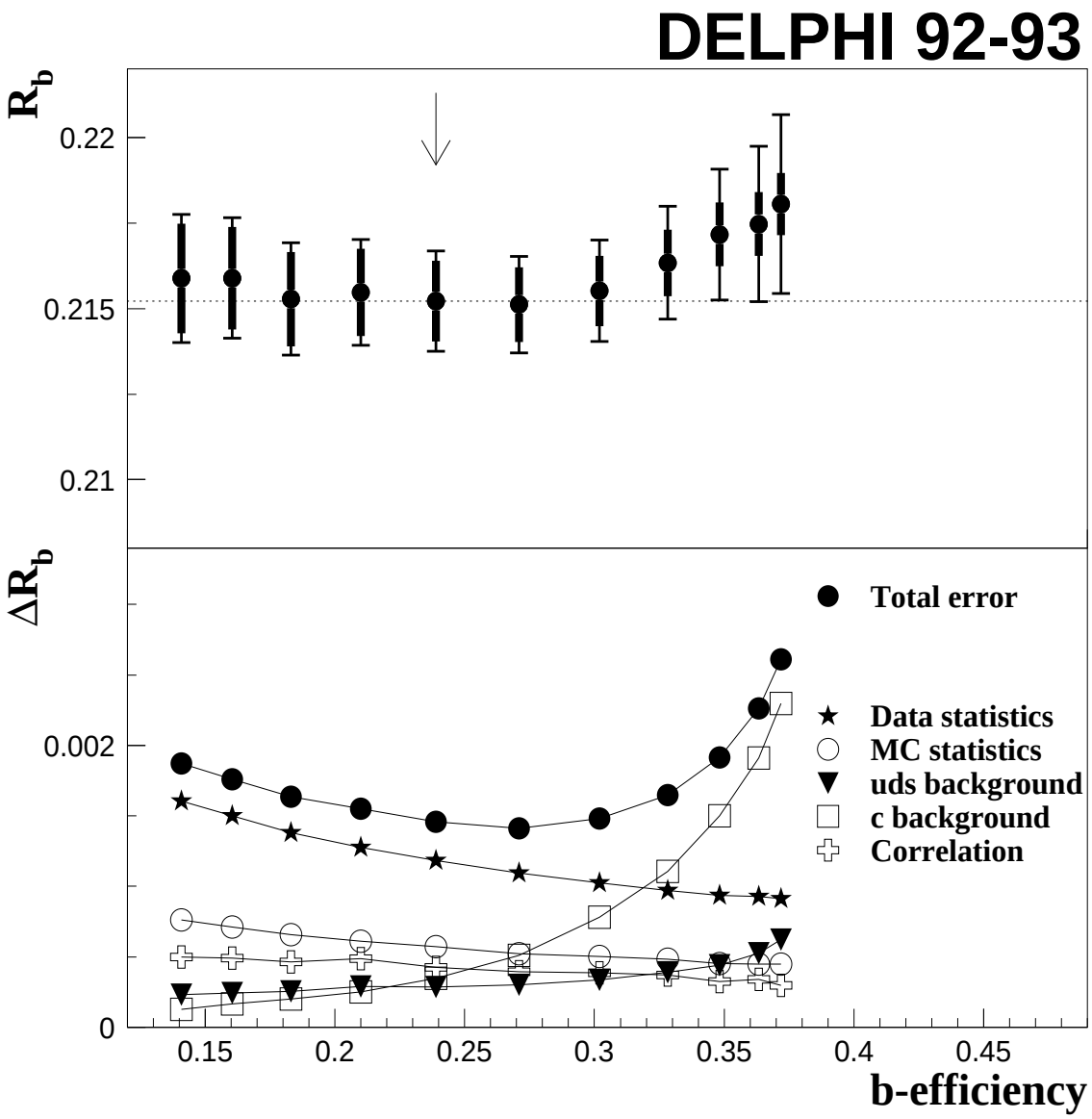

Figure 10: Stability of the 1992–1993 R_b result as a function of the b-tight tag efficiency, together with the contributions to the total error. The working point is chosen to have a similar purity to that at the working point of the 1994–1995 analysis. It results in an efficiency of 23.9% with a b-purity of 98.2%.

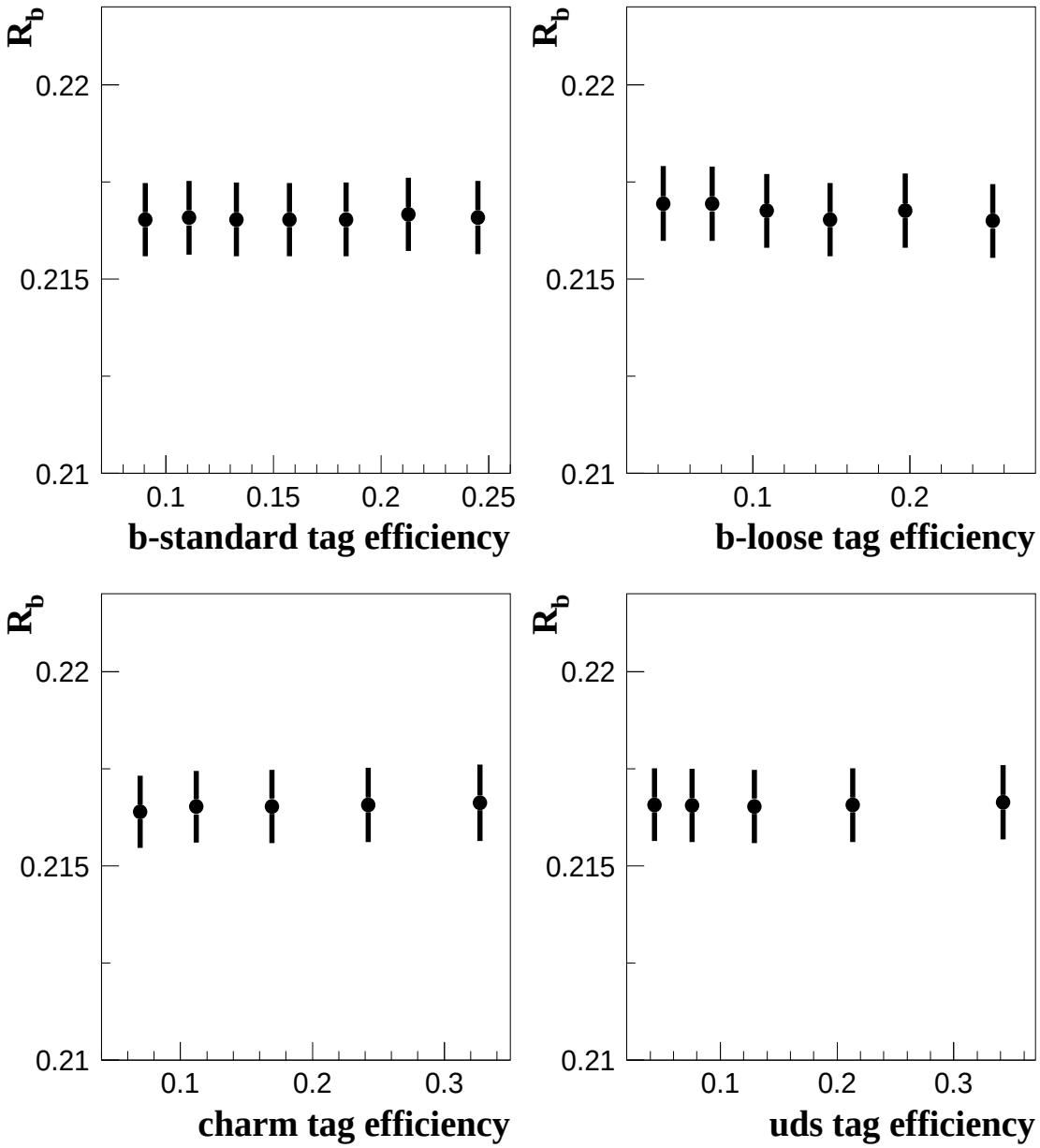

Figure 11: Stability of the R_{b} result as a function of the efficiencies of the b-standard, b-loose, charm and uds hemisphere tags for 1994–1995. Only the data and simulation statistical errors are shown.

	$\Delta R_{\rm b} \times 10^4$				
Error Source	1992	1993	1994	1995	Comb.
Statistical error	± 16.4	± 17.1	± 9.9	± 14.5	± 6.7
Simulation statistics	± 8.7	± 7.6	± 4.4	± 8.2	± 3.2
Light quark efficiency	± 2.8	± 2.9	± 3.1	± 2.7	± 3.0
Charm efficiency	± 3.4	± 3.6	± 2.8	± 3.1	± 3.1
Angular correlation	± 2.7	± 2.7	± 0.6	± 1.5	± 0.9
Gluon radiation	± 2.4	± 2.4	± 2.7	± 2.7	± 2.6
Physics correlation	± 2.5	± 2.5	± 1.4	± 1.4	± 1.7
Acceptance bias	± 2.3	± 1.8	± 1.3	± 2.2	± 0.9
Total systematic error	± 10.9	± 10.0	± 6.9	± 10.1	± 6.1
Total	± 19.7	± 19.8	± 12.1	± 17.5	± 9.1

Table 11: Sources of error for the measurement of $R_{\rm b}$ using the Multivariate Analysis on all data sets and the combination.

6.1 Secondary vertex search

The search for secondary vertices was made independently inside event hemispheres defined by the plane perpendicular to the event thrust axis. Hemisphere tracks used in the analysis were required to fulfil the following criteria to ensure precise tracks:

- $R\phi$ hits in at least 2 layers of the VD,
- an impact parameter in the $R\phi$ plane with respect to the beam-spot of less than 0.15 cm,
- a momentum greater than 750 MeV/c.

In addition K^0_S and Λ particles and photon conversions were reconstructed, details of which are given in [10]. Tracks coming from the decay of a K^0_S or Λ or from a photon conversion were rejected.

Candidate secondary vertices were identified by the following procedure.

- All possible three-track vertices in the $R\phi$ plane were found. Candidates were rejected if any of the following conditions was met: i) the decay length, L, to the beam-spot was smaller than σ_L, where σ_L is the uncertainty on L; ii) $L > 3.0$ cm; and iii) the χ^2 probability for forming a vertex out of these tracks, $P(\chi^2)$, was less than 1%.
- Next, an attempt was made to add to candidate vertices any track likely to have originated from the same point in space. Each track falling within a cone of half-angle 0.4 radian placed around the candidate vertex momentum vector was fitted in turn to the vertex. That track which contributed the largest increase in L/σ_L was added permanently to the candidate vertex provided that: i) $L > 3\sigma_L$; ii) $L < 3.0$ cm; and iii) $P(\chi^2) > 1\%$. This procedure was continued until no more tracks could be added.

- In an attempt to identify cascade decays, $b \to c$, where the b and c vertices are significantly separated, further tracks were added to the vertex if they were deemed to be consistent, within the errors, with the candidate while at the same time inconsistent with the beam-spot.

- Finally, using a procedure similar to that outlined above, a single primary vertex per hemisphere was found from tracks that were consistent with the beam-spot position. A *unique* track was defined to be one that was included in a candidate secondary vertex but was not part of the primary vertex. Secondary vertex candidates that did not contain a unique track were removed.

Close attention was paid to reducing light quark backgrounds, which are most sensitive to the modelling of the tracking in the simulation. For the case of vertices containing two unique tracks that included z-hits, these two tracks were separately fitted to form a three-dimensional vertex point. Requiring $P(\chi^2) > 0.1\%$ was found to be an effective cut for removing cases where badly reconstructed tracks might form a vertex in two dimensions but were clearly unassociated with each other once the z-coordinate was considered. Note that this procedure was only possible for data taken with the three-dimensional VD, i.e. from 1994 onwards.

If after the secondary vertex finding procedure there was more than one candidate vertex in a hemisphere, the vertex containing the largest number of unique tracks was chosen to tag the hemisphere.

6.2 Tagging $Z \to b\bar{b}$ events

In order to tag $Z \to b\bar{b}$ events, the output of a neural network [28] was used with five input variables derived from the properties of the reconstructed vertices. The neural network was trained using 5000 $b\bar{b}$ and 5000 $(u\bar{u} + d\bar{d} + s\bar{s} + c\bar{c})$ simulated events.

The input variables were

1. the number of unique tracks in the secondary vertex;

2. the number of tracks in the primary vertex that were not also associated to a secondary;

3. the number of tracks in common to both the secondary and primary vertices;

4. the decay length significance L/σ_L;

5. the secondary vertex rapidity, defined as

$$R = \ln \frac{E + P_{\parallel}}{\sqrt{m_0^2 + {P_t}^2}}, \tag{16}$$

where E is the energy, m_0 the invariant mass, P_t the summed absolute transverse momenta and $P_{\parallel}$ the summed longitudinal momenta of unique tracks in the vertex with respect to the jet axis.

Distributions of all input variables and the resulting neural network output for simulation and data are shown in figure 12.

The calculation of R_b followed the double hemisphere method described in section 4.

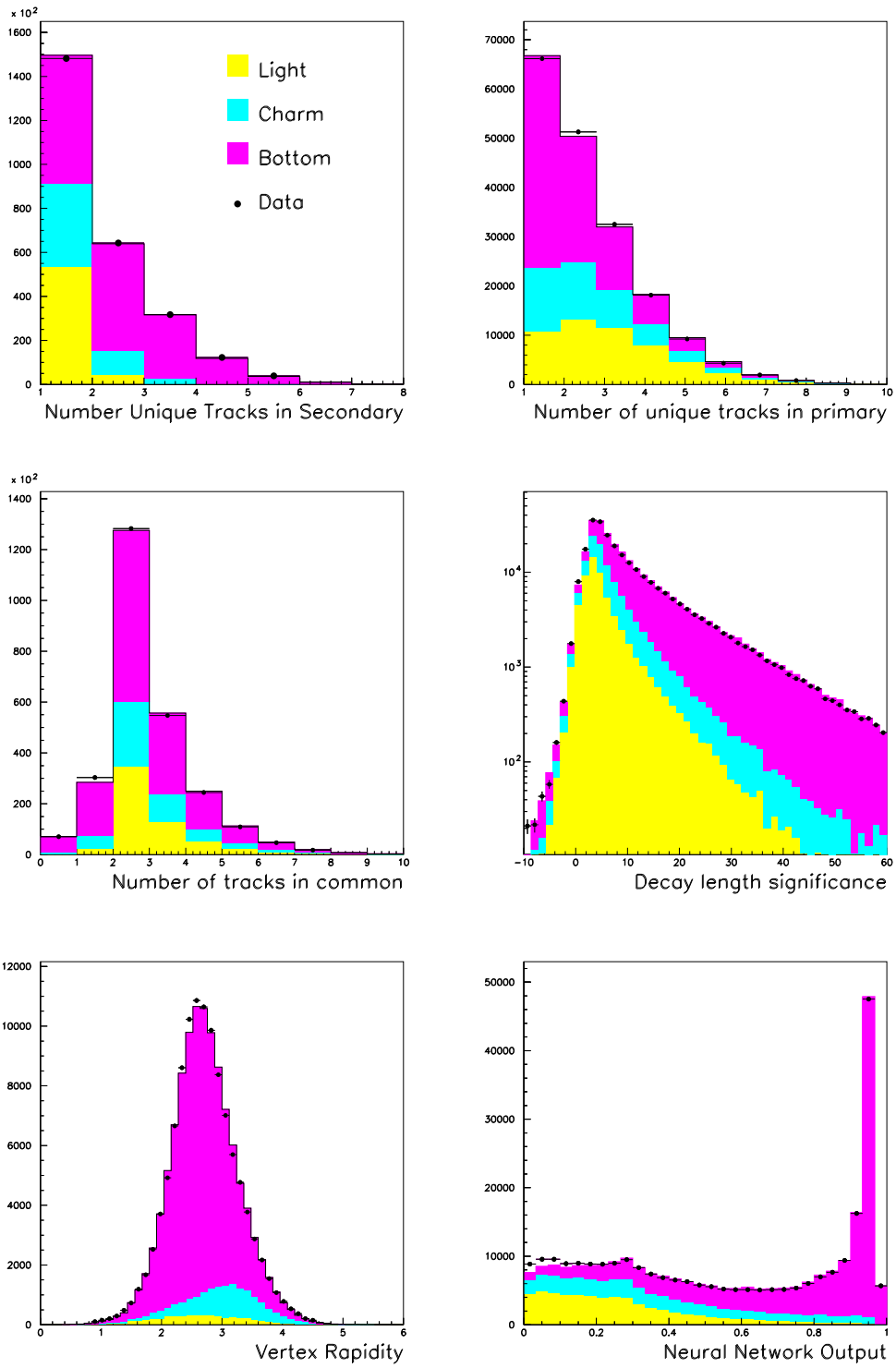

Figure 12: Distributions comparing data and simulation for the 5 input variables to the neural network and for the neural network output itself.

6.3 Quantities from the simulation

Both the light and charm quark efficiencies were extracted from the simulation with reweighting to reach the input values of various modelling parameters recommended in [18] and listed in table 12. This took account of the rate of gluon splitting to heavy quarks in light quark events, and in the charm sector of differences between the parameters used in the simulation and experimentally measured values of the charmed hadron lifetimes, production fractions and decay modes and charm fragmentation. Further reweighting to the experimental limits was carried out to estimate the uncertainties on these efficiencies, which are shown in table 12 along with the small uncertainty due to limited simulation statistics and an error coming from details of the modelling of DELPHI detector tracking in the simulation. This uncertainty due to detector effects was estimated in a similar way to that described in section 4.3. It should be noted that the simulation sample used to train the neural network was excluded from that used in the determination of background efficiencies.

Source of error	Range	$\Delta\epsilon_{uds} \times 10^5$			
		1992	1993	1994	1995
Simulation statistics		$\pm$ 2.9	$\pm$ 2.6	$\pm$ 2.1	$\pm$ 2.6
Detector effects		$\pm$ 2.8	$\pm$ 3.1	$\pm$ 2.5	$\pm$ 2.6
$g \to c\bar{c}$	(2.33 $\pm$ 0.50)%	$\pm$ 2.8	$\pm$ 3.9	$\pm$ 3.8	$\pm$ 2.9
$g \to b\bar{b}$	(0.269$\pm$ 0.067)%	$\pm$ 6.0	$\pm$ 5.5	$\pm$ 6.3	$\pm$ 5.7
Light hadron modelling	Tuned JETSET $\pm$ 10%	$\pm$ 3.4	$\pm$ 5.0	$\pm$ 4.9	$\pm$ 5.0
		$\Delta\epsilon_c \times 10^4$			
Simulation statistics		$\pm$ 2.0	$\pm$ 1.7	$\pm$ 1.5	$\pm$ 1.7
Detector effects		$\pm$ 4.1	$\pm$ 4.2	$\pm$ 3.9	$\pm$ 3.3
$\langle x_E(\mathrm{c}) \rangle$	0.484 $\pm$ 0.008	$\mp$ 2.1	$\mp$ 2.1	$\mp$ 2.8	$\mp$ 2.6
D^+ fraction	0.233 $\pm$ 0.027	$\pm$ 4.0	$\pm$ 4.3	$\pm$ 3.9	$\pm$ 3.5
D_s fraction	0.103 $\pm$ 0.029	$\pm$ 0.7	$\pm$ 0.6	$\pm$ 0.5	$\pm$ 0.5
c-baryon fraction	0.063 $\pm$ 0.028	$\mp$ 2.7	$\mp$ 2.6	$\mp$ 2.4	$\mp$ 2.1
D^0 lifetime	0.415 $\pm$ 0.004 ps	$\pm$ 1.0	$\pm$ 0.9	$\pm$ 0.9	$\pm$ 0.8
D^+ lifetime	1.057 $\pm$ 0.015 ps	$\pm$ 0.6	$\pm$ 0.6	$\pm$ 0.6	$\pm$ 0.5
D_s lifetime	0.467 $\pm$ 0.017 ps	$\pm$ 0.6	$\pm$ 0.6	$\pm$ 0.6	$\pm$ 0.5
Λ_c lifetime	0.206 $\pm$ 0.012 ps	$\pm$ 1.1	$\pm$ 0.2	$\pm$ 0.6	$\pm$ 0.0
D decay multiplicity	as LEPHF	$\pm$ 3.5	$\pm$ 3.5	$\pm$ 3.2	$\pm$ 2.9
BR($\mathrm{D}^0 \to$ no neutrals)	0.141 $\pm$ 0.011	$\pm$ 1.4	$\pm$ 1.4	$\pm$ 1.4	$\pm$ 1.1
BR($\mathrm{D}^1 \to$ 1 neut., $\geq$ 2 charged)	0.377 $\pm$ 0.017	$\pm$ 0.3	$\pm$ 0.3	$\pm$ 0.3	$\pm$ 0.3
BR($\mathrm{D}^+ \to$ no neutrals)	0.112 $\pm$ 0.006	$\pm$ 0.7	$\pm$ 0.7	$\pm$ 0.7	$\pm$ 0.6
BR($\mathrm{D}^+ \to$ 1 neut., $\geq$ 2 charged)	0.261 $\pm$ 0.023	$\pm$ 1.8	$\pm$ 1.9	$\pm$ 1.7	$\pm$ 1.5
BR($\mathrm{D}_s \to \mathrm{K}^0\mathrm{X}$)	0.33 $\pm$ 0.18	$\mp$ 1.0	$\mp$ 0.9	$\mp$ 0.7	$\mp$ 0.5

Table 12: Contributions to the systematic uncertainties on the efficiencies for tagging light and charm quarks, as estimated from the simulation.

The various sources of systematic error are shown in the lower half of figure 13, together with the statistical and total errors, as a function of the efficiency for identifying b quarks in the 1994 data set. The arrow in the upper half indicates the working point where the minimum total error is found. At this point, taking 1994 data as an example, the b-purity in the simulation was 94.8% for a b-tagging efficiency of 26.4%, to be compared with an efficiency of 28.2 $\pm$ 0.2% calculated from the data. The same cut on the neural network

output was used for each data set and resulted in similar b-tagging performances.

The light and charm quark efficiencies extracted from the 1994 simulation at the working point were:

$$\begin{aligned} \epsilon_{\rm uds} &= (0.100 \pm 0.009) \times 10^{-2} \\ \epsilon_{\rm c} &= (1.35 \pm 0.08) \times 10^{-2} \end{aligned} \tag{17}$$

and their contributions to the systematic error on $R_{\rm b}$ are summarised in table 13, together with the results for 1992, 1993 and 1995.

Correlations between hemispheres come from both geometrical and kinematic effects, as described in section 4.4. The hemisphere correlation in b events for this analysis was estimated from the 1994 simulation to be

$$\rho = (0.53 \pm 0.21(\text{stat}) \pm 0.08(\text{syst})) \times 10^{-2}, \tag{18}$$

with similar values obtained for the other data sets. The first error is due to the limited simulation statistics and the second is the estimated systematic uncertainty. Contributions to the systematic error from both geometrical effects and physics modelling, for each of the years, are estimated as described in section 4.4 and the resulting uncertainties on the measurement of $R_{\rm b}$ are summarised in table 13.

6.4 Results

Using the numbers of data events with one and with both hemispheres tagged and the values for the efficiencies and correlations of which examples are given above, and taking into account the selection bias towards $\mathrm{Z} \to \mathrm{b\overline{b}}$ events, $R_{\rm b}$ was calculated separately in each data set to be:

$$\begin{aligned} R_{\rm b} &= 0.21746 \pm 0.00192(\text{stat}) \pm 0.00150(\text{syst}) - 0.093(R_{\rm c} - 0.172) \quad (1992) \\ R_{\rm b} &= 0.21830 \pm 0.00189(\text{stat}) \pm 0.00138(\text{syst}) - 0.089(R_{\rm c} - 0.172) \quad (1993) \\ R_{\rm b} &= 0.21609 \pm 0.00138(\text{stat}) \pm 0.00120(\text{syst}) - 0.087(R_{\rm c} - 0.172) \quad (1994) \\ R_{\rm b} &= 0.21835 \pm 0.00221(\text{stat}) \pm 0.00153(\text{syst}) - 0.082(R_{\rm c} - 0.172) \quad (1995). \end{aligned}$$

The stability of the measurement over a range of b-tagging efficiencies can be seen in the upper half of figure 13, again taking 1994 as an example.

Assuming all physics modelling uncertainties to be fully correlated between the different data sets and all statistical and detector effects to be totally uncorrelated, the results were combined to give a final value for the 1992–1995 data sets of

$$R_{\rm b} = 0.21717 \pm 0.00089(\text{stat}) \pm 0.00112(\text{syst}) - 0.088(R_{\rm c} - 0.172).$$

The full breakdown of the uncertainties on the combined result is given in table 13.

7 Energy Dependence

In 1993 and 1995, data were taken at three different centre of mass energies ($\sqrt{s}$ = 89.46, 91.27, 93.00 GeV). As photon exchange and $\gamma - \mathrm{Z}$ interference are strongly suppressed at energies close to the Z resonance, $R_{\rm b}(\sqrt{s})$ is predicted to be almost constant in

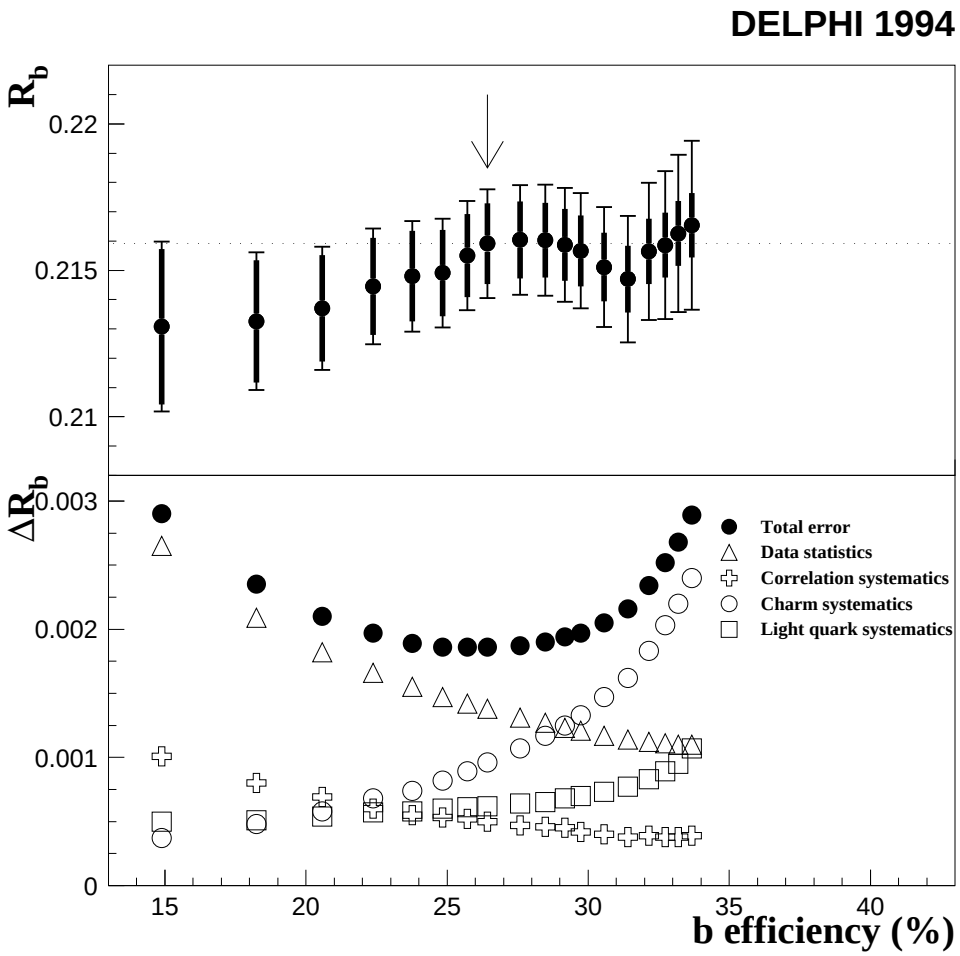

Figure 13: The measured value of R_{b} from the 1994 data set as a function of the b-tagging efficiency taken from the simulation, together with the contributions to the total uncertainty on R_{b}. In the upper plot, the thick error bars show the statistical errors, the thinner bars indicate the total errors, and all errors are correlated from point to point. The arrow marks the position of the cut and the line shows the value at that cut.

Source of error	$\Delta R_b \times 10^4$				
	1992	1993	1994	1995	Comb.
Statistical error	$\pm$ 19.2	$\pm$ 18.9	$\pm$ 13.8	$\pm$ 22.1	$\pm$ 8.9
Simulation statistics	$\pm$ 8.9	$\pm$ 6.4	$\pm$ 4.9	$\pm$ 9.0	$\pm$ 3.4
Light quark efficiency	$\mp$ 3.5	$\mp$ 3.7	$\mp$ 4.0	$\mp$ 4.0	$\mp$ 3.7
Charm quark efficiency	$\mp$ 9.8	$\mp$ 9.6	$\mp$ 9.6	$\mp$ 9.2	$\mp$ 8.7
Angular correlation	$\pm$ 4.7	$\pm$ 5.4	$\pm$ 1.6	$\pm$ 6.4	$\pm$ 3.7
Gluon radiation	$\pm$ 3.2	$\pm$ 3.2	$\pm$ 3.0	$\pm$ 3.0	$\pm$ 3.1
b physics correlation	$\pm$ 0.9	$\pm$ 1.0	$\pm$ 0.5	$\pm$ 0.5	$\pm$ 0.6
Acceptance bias	$\pm$ 1.8	$\pm$ 1.8	$\pm$ 0.2	$\pm$ 1.3	$\pm$ 0.6
Total systematic error	$\pm$ 15.0	$\pm$ 13.8	$\pm$ 12.0	$\pm$ 15.3	$\pm$ 11.2
Total error	$\pm$ 24.3	$\pm$ 23.4	$\pm$ 18.3	$\pm$ 26.9	$\pm$ 14.3

Table 13: Summary of the systematic uncertainties on R_b from the Secondary Vertex Analysis, for all data sets and for the combined result.

the Standard Model. However, if R_b is affected by the interference of the Z with another particle like a Z′ [29] which is almost degenerate in mass, some energy dependence can be expected if the mass and width of the Z' are not exactly equal to those of the Z. Similar effects could arise from an R-parity violating sneutrino [30].

Since the b-tagging efficiency varies only very little within the energy range considered here, no complicated single to double tag comparison is needed to measure $\frac{R_b(\sqrt{s})}{R_b(91.27\,\mathrm{GeV})}$. Instead, simply the ratio of the fraction of tagged events can be used, with very small corrections due to changes in the b-tagging efficiency and almost negligible corrections due to background. These corrections were calculated using the simulation. The measurement was performed using event lifetime probabilities which result in a much higher efficiency for a given purity than hemisphere probabilities. Several different values of the event probability cut were used, and a minimum statistical error was found at a b-purity of 85%. At this value of the cut, the b-tagging efficiency was consistent with being independent of energy within the simulation statistical error of typically 0.2%. It was about 75% (81%) for 1993 (1995), while the efficiency to tag c and uds events was about 11% (13%) and 1.6% (1.4%). The following ratios were found:

$$R_- = \frac{R_b(89.46\,\mathrm{GeV})}{R_b(91.27\,\mathrm{GeV})} = 0.9909 \pm 0.0081$$
$$R_+ = \frac{R_b(93.00\,\mathrm{GeV})}{R_b(91.27\,\mathrm{GeV})} = 1.0069 \pm 0.0069.$$

The error is statistical only. All systematic uncertainties were found to be negligible. The values are consistent with the Standard Model prediction of 0.997 (0.998) for R_- (R_+). Figure 14 shows the stability of the measurement as a function of the b-purity for the two years of data taking.

8 Results and Discussion

Three different measurements of the partial decay width R_b^0 of the Z into B-hadrons have been performed. Events were selected using tracks having large impact parameters in jets

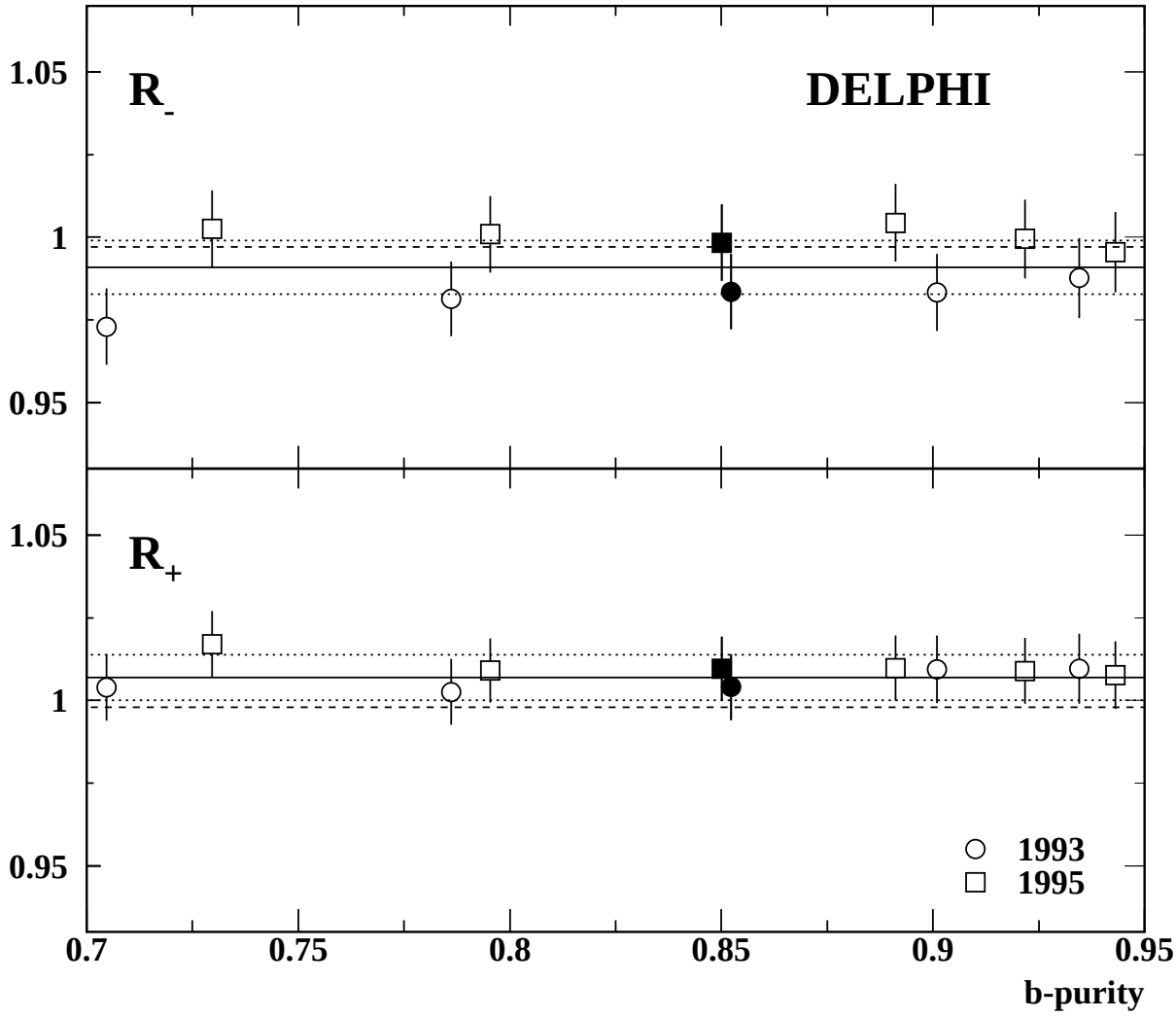

Figure 14: Ratio of the off-peak and on-peak R_{b} values as a function of the b-purity. The closed points represent the point of minimal error which have been used for the central result. The solid lines represent the average over the two years with its error indicated by the dotted lines. The dashed lines indicate the Standard Model expectation.

with reconstructed secondary vertices or with a multivariate technique or with a neural network method for secondary vertices.

The Enhanced Impact Parameter Analysis compares single and double tag rates to extract R_{b}, using a highly efficient and pure b-tag. The enhanced impact parameter tag of this analysis is then used as the primary b-tag in the Multivariate Analysis, which includes additional tags for b-, c- and light quarks. The information of the first analysis is therefore fully included in the second one and no further combination is possible.

Using a Monte Carlo technique, the statistical correlation between the Multivariate and the Secondary Vertex Analyses has been evaluated to be less than 26% (39%) at 90% C.L. for the 1994–1995 (1992–1993) analysis. Since the results are statistically consistent and not strongly correlated they could be combined, taking into account all sources of correlation. In the combination the result does not improve with respect to the Multivariate Analysis alone and so this is the final result of this paper and the Secondary Vertex Analysis is used as a cross-check.

Using about 3.4 million hadronic events collected in the years 1992–1995 by DELPHI and combining all centre of mass energies at which LEP has run, the following result was obtained with the Multivariate Analysis:

$$R_{\mathrm{b}} = 0.21605 \pm 0.00067(\mathrm{stat}) \pm 0.00061(\mathrm{syst}) - 0.024(R_{\mathrm{c}} - 0.172).$$

Applying the small (+0.00020) correction for photon exchange yields for the ratio of partial widths:

$$R^0_{\mathrm{b}} = 0.21625 \pm 0.00067(\mathrm{stat}) \pm 0.00061(\mathrm{syst}) - 0.024(R_{\mathrm{c}} - 0.172).$$

The detailed error breakdown of the error for this measurement as well as for each year of operation is given in table 14.

Using the same data set, the Secondary Vertex Analysis can be used as an independent cross-check of the Multivariate Analysis. The result was:

$$R^0_{\mathrm{b}} = 0.21737 \pm 0.00089(\mathrm{stat}) \pm 0.00112(\mathrm{syst}) - 0.088(R_{\mathrm{c}} - 0.172).$$

The result is in agreement with those of other measurements at LEP [3, 4, 6, 7, 8]. It is also in good agreement with the Standard Model expectation of $R^0_{\mathrm{b}} = 0.21548 \mp 0.00018$ [31], assuming a mass of the top quark of $m_t = 173.8 \pm 5.2\ GeV/c^2$ [21].

Acknowledgements

We are greatly indebted to our technical collaborators and to the funding agencies for their support in building and operating the DELPHI detector, and to the members of the CERN-SL Division for the excellent performance of the LEP collider.

Source of error	Range	$\Delta R_b \times 10^4$ 1992	1993	1994	1995	Comb.
Data statistics		$\pm$ 16.39	$\pm$ 17.05	$\pm$ 9.92	$\pm$ 14.46	$\pm$ 6.74
Simulation statistics		$\pm$ 8.69	$\pm$ 7.56	$\pm$ 4.39	$\pm$ 8.23	$\pm$ 3.21
Event selection		$\pm$ 2.25	$\pm$ 1.79	$\pm$ 1.27	$\pm$ 2.24	$\pm$ 0.87
Tracking		$\pm$ 2.06	$\pm$ 2.16	$\pm$ 1.53	$\pm$ 1.78	$\pm$ 1.29
K^0, Λ^0, photons, etc.	see text	$\pm$ 0.69	$\pm$ 0.70	$\pm$ 0.30	$\pm$ 0.27	$\pm$ 0.42
Gluon splitting $g \to c\bar{c}$	$(2.33 \pm 0.50)\%$	$\pm$ 0.63	$\pm$ 0.63	$\pm$ 0.95	$\pm$ 0.85	$\pm$ 0.83
Gluon splitting $g \to b\bar{b}$	$(0.269 \pm 0.067)\%$	$\pm$ 2.63	$\pm$ 2.67	$\pm$ 2.80	$\pm$ 2.50	$\pm$ 2.70
D^+ fraction in $c\bar{c}$ events	0.233 ± 0.027	$\pm$ 1.14	$\pm$ 1.20	$\pm$ 1.24	$\pm$ 1.31	$\pm$ 1.24
D_s fraction in $c\bar{c}$ events	0.103 ± 0.029	$\mp$ 0.28	$\mp$ 0.28	$\mp$ 0.26	$\mp$ 0.26	$\mp$ 0.27
c-baryon fraction in $c\bar{c}$ events	0.063 ± 0.028	$\mp$ 1.33	$\mp$ 1.39	$\mp$ 1.13	$\mp$ 1.19	$\mp$ 1.22
BR($D^0 \to$ no neutrals)	$(14.1 \pm 1.1)\%$	$\pm$ 0.56	$\pm$ 0.60	$\pm$ 0.62	$\pm$ 0.66	$\pm$ 0.62
BR($D^0 \to$ 1 neut., $\geq$ 2 charged)	$(37.7 \pm 1.7)\%$	$\pm$ 0.28	$\pm$ 0.30	$\pm$ 0.25	$\pm$ 0.26	$\pm$ 0.27
BR($D^+ \to$ no neutrals)	$(11.2 \pm 0.6)\%$	$\pm$ 0.42	$\pm$ 0.45	$\pm$ 0.50	$\pm$ 0.52	$\pm$ 0.49
BR($D^+ \to$ 1 neut., $\geq$ 2 charged)	$(26.1 \pm 2.3)\%$	$\pm$ 0.28	$\pm$ 0.30	$\pm$ 0.13	$\pm$ 0.13	$\pm$ 0.18
BR($D_s \to K^0X$)	$(33 \pm 18)\%$	$\pm$ 1.13	$\pm$ 1.19	$\pm$ 1.24	$\pm$ 1.31	$\pm$ 1.23
D^0 lifetime	0.415 ± 0.004 ps	$\pm$ 0.28	$\pm$ 0.30	$\pm$ 0.25	$\pm$ 0.26	$\pm$ 0.27
D^+ lifetime	1.057 ± 0.015 ps	$\pm$ 0.28	$\pm$ 0.30	$\pm$ 0.25	$\pm$ 0.26	$\pm$ 0.27
D_s lifetime	0.447 ± 0.017 ps	$\pm$ 0.28	$\pm$ 0.30	$\pm$ 0.25	$\pm$ 0.26	$\pm$ 0.27
Λ_c lifetime	0.206 ± 0.012 ps	$\pm$ 0.00	$\pm$ 0.00	$\pm$ 0.00	$\pm$ 0.00	$\pm$ 0.00
D decay multiplicity	see [18]	$\pm$ 1.17	$\pm$ 1.22	$\pm$ 0.64	$\pm$ 0.67	$\pm$ 0.82
$\langle x_E(c) \rangle$	0.484 ± 0.008	$\pm$ 0.47	$\pm$ 0.50	$\pm$ 0.54	$\pm$ 0.56	$\pm$ 0.53
Two b's same hemisphere	$\pm 30\%$	$\pm$ 0.66	$\pm$ 0.66	$\pm$ 0.44	$\pm$ 0.44	$\pm$ 0.51
$\langle x_E(b) \rangle$	0.702 ± 0.008	$\pm$ 1.77	$\pm$ 1.77	$\pm$ 1.00	$\pm$ 1.00	$\pm$ 1.24
B decay multiplicity	4.97 ± 0.07	$\mp$ 1.46	$\mp$ 1.46	$\mp$ 0.65	$\mp$ 0.65	$\mp$ 0.91
Average B lifetime	1.55 ± 0.05 ps	$\mp$ 0.03	$\mp$ 0.03	$\mp$ 0.03	$\mp$ 0.03	$\mp$ 0.03
Angular effects (correl.)	see text	$\pm$ 2.27	$\pm$ 2.35	$\pm$ 0.20	$\pm$ 1.20	$\pm$ 0.81
Angular effects (uncorrel.)	see text	$\pm$ 1.40	$\pm$ 1.40	$\pm$ 0.61	$\pm$ 0.94	$\pm$ 0.46
Gluon radiation	see text	$\pm$ 2.38	$\pm$ 2.38	$\pm$ 2.65	$\pm$ 2.65	$\pm$ 2.57
Total systematic error		$\pm$ 10.86	$\pm$ 9.98	$\pm$ 6.87	$\pm$ 10.03	$\pm$ 6.12
Total error		$\pm$ 19.66	$\pm$ 19.75	$\pm$ 12.06	$\pm$ 17.60	$\pm$ 9.11

Table 14: Detailed error breakdown for the measurement of R_b from the Multivariate Analysis, for all data sets and the combination.

References

[1] The LEP Collaborations and SLD, *A Combination of Preliminary Electroweak Measurements and Constraints on the Standard Model*, CERN-PPE/97-154.

[2] J. Ellis, J. L. Lopez, and D. V. Nanopoulos, Phys. Lett. **B397** (1997) 88.

[3] ALEPH Collaboration, R. Barate et al., Phys. Lett.**B401** (1997) 150.

[4] ALEPH Collaboration., R. Barate et al., Phys. Lett. **B401** (1997) 163.

[5] DELPHI Collaboration, P. Abreu et al., Z. Phys. **C70** (1996) 531.
DELPHI Collaboration, P. Abreu et al., Z. Phys. **C66** (1995) 323.

[6] L3 Collaboration, O. Adriani et al., Phys. Lett. **B307** (1993) 237.

[7] OPAL Collaboration, K.Ackerstaff et al., Z. Phys. **C74** (1997) 1.

[8] SLD Collaboration, SLAC-PUB-7481 (to be submitted to Phys. Rev. Lett.)

[9] DELPHI Collaboration, P. Aarnio et al., Nucl. Inst. Meth. **A303** (1991) 233.

[10] DELPHI Collaboration, P. Abreu et al., Nucl. Inst. Meth. **A378** (1996) 57.

[11] N. Bingefors et al., Nucl. Inst. Meth. **A328** (1993) 447.

[12] V. Chabaud et al., Nucl. Inst. Meth **A368** (1996) 314.

[13] T. Sjöstrand et al., in *"Z physics at LEP 1"*, CERN 89-08, CERN, Geneva, 1989; Comp. Phys. Comm. **39** (1986) 347.

[14] G. Borisov and C. Mariotti, Nucl. Inst. Meth. **A372** (1996) 181.
G. Borisov and C. Mariotti, *Tuning of the Track Impact Parameter Resolution of the Upgraded DELPHI Detector*, ISS-INFN 97/14 (also DELPHI note, DELPHI 97-95 PHYS 717.

[15] G. Borisov, *Combined b-tagging*, DELPHI note, DELPHI 97-94 PHYS 716.

[16] ALEPH Collaboration, D. Buskulic et al., Phys. Lett. **B313** (1993), 535.

[17] G.V.Borisov, *Lifetime Tag of Events with B-hadrons with the DELPHI Detector*, preprint IHEP (Protvino), 94-98 (1994).

[18] The LEP Collaborations Nucl. Inst. Meth. A378 (1996) 101;
The LEP Heavy Flavour Working Group , *Presentation of LEP Electroweak Heavy Flavour Result for Summer 1996 Conferences*, LEPHF 96-01.

[19] ALEPH Collaboration, R. Barate et al., *A measurement of the Gluon Splitting Rate into* $b\bar{b}$ *Pairs in Hadronic Z decays*, CERN-EP/98-103 (submitted to Phys. Lett. B).
DELPHI Collaboration, P. Abreu et al., Phys. Lett. **B405** (1997) 202.

[20] LEP collaboration and SLD,*Input parameters for the LEP electroweak Heavy Flavour Results for Summer 1998 Conferences*, LEPHF/98-01.

[21] The Particle Data Group, C. Caso et al., E. Phys. J. **C3** (1998) 1

[22] DELPHI Collaboration, P. Abreu et al., Phys. Lett. **B425** (1998) 399.

[23] A.G. Frodesen, O. Skeggestad and H. Tofte, *Probability and statistics in particle physics*, Universitetsforlaget 1979.

[24] NAGLIB Manual. CERN Program Library.

[25] P. Billoir et al., Nucl. Inst. Meth. **A360** (1995) 532.

[26] F. Martínez-Vidal, *High precision measurement of* $\Gamma(Z \to b\bar{b})/\Gamma(Z \to hadrons)$ *with the DELPHI detector at LEP collider*, Ph.D. Thesis, Universitat de València, ISBN 84-370-3406-X and CERN-THESIS-98-002.

[27] W.J. Murray, *Improved B tagging using impact parameters*, internal DELPHI Note, DELPHI 95-167 PHYS 581.

[28] A. Zell et al., *Stuttgart Neural Network Simulator*, University of Stuttgart, Institute for Parallel and Distributed High Performance Systems.

[29] F. Caravaglios and G. Ross, Phys. Lett. **B346** (1995) 159.

[30] J. Erler, J. L. Feng, and N. Polonsky, Phys. Rev. Lett. **78** (1997) 3063.

[31] D. Bardine et al., *ZFITTER: An Analytical Program for Fermion Pair Production in* e^+e^- *Annihilation*, CERN-TH 6443/92 (May 1992).